A11102 717695

NBS
PUBLICATIONS

NBSIR 87-3618

Computer Software for the Computation of the Scattered Field and the Optical Microscope Image of Line Objects Patterned in Thick Layers

D. Nyyssonen

CD Metrology, Inc.
Germantown, MD 20874

December 1987

Prepared for:
U.S. DEPARTMENT OF COMMERCE
National Bureau of Standards
National Engineering Laboratory
...r Manufacturing Engineering
... Engineering Division
...burg, MD 20899

QC
100
.U56
87-3618
1987
C.2

Research Information Center
National Bureau of Standards
Gaithersburg, Maryland 20899

NBSIR 87-3618

COMPUTER SOFTWARE FOR THE COMPUTATION OF THE SCATTERED FIELD AND THE OPTICAL MICROSCOPE IMAGE OF LINE OBJECTS PATTERNED IN THICK LAYERS

D. Nyyssonen

CD Metrology, Inc.
Germantown, MD 20874

December 1987

Prepared for:
U.S. DEPARTMENT OF COMMERCE
National Bureau of Standards
National Engineering Laboratory
Center for Manufacturing Engineering
Precision Engineering Division
Gaithersburg, MD 20899

U.S. DEPARTMENT OF COMMERCE, C. William Verity, *Secretary*
NATIONAL BUREAU OF STANDARDS, Ernest Ambler, *Director*

Table of Contents

	Page
Abstract	1
Introduction	1
Software Structure	3
Implementation and Testing	5
Accuracy	6
Acknowledgments	7
References	7
Table	9
Appendix I	10
Appendix II	30
Appendix III	52

Computer Software for the Computation of the Scattered Field and the Optical Microscope Image of Line Objects Patterned in Thick Layers

Diana Nyyssonen
CD Metrology, Inc.
Germantown, MD 20874

ABSTRACT: This report contains computer software for calculating optical microscope images of line objects patterned in thick layers (>λ/4 thick). The algorithms used are based on a monochromatic, waveguide model which can predict the images of line objects with arbitrary edge geometry including multilayer structures with sloped, curved, asymmetric, and undercut edges. Along with the computer software listing, the mathematics of the model, a short description of its structure and use, and test cases for help in implementation are given.

KEY WORDS: computer software; diffraction; dimensional metrology; linewidth; microscopy; optical imaging; optical metrology.

INTRODUCTION

The computer software described in this report was written in conjunction with the NBS project to develop fundamentally accurate optical measurement techniques for the width of micrometer and submicrometer lines patterned on integrated circuit wafers. Accurate and precise measurement techniques for linewidth are needed to improve yield, to ensure that lithographic and critical dimension (CD) measurement systems meet specification, to establish control of fabrication processes, and as input to device modeling and simulation programs.

In the course of research and development of the NBS laser linewidth measurement system [1], it was found that the microscope

image profiles for lines patterned in thick layers (>λ/4 thick) were not properly predicted by the scalar theory conventionally used to calculate images of line objects [2, 3]. Scalar imaging theory assumes that the object is planar (thin compared to the wavelength of the illumination) and can be represented by a complex transmittance or reflectance function. The scalar model does not take into account the multiple reflections or standing waves that may occur within the patterned layer or the edge effects that occur in thick layers.

A new model was developed by Nyyssonen [4, 5] based on a waveguide approach which characterizes the patterned layer by its complex dielectric constant and calculates the waveguide modes supported by the line structure. First, the mode expansion of the electromagnetic fields within the patterned layer is found and then the appropriate boundary conditions are used to calculate the scattered field.

Nyyssonen's model assumes that the line structure is patterned in a nonmagnetic layer which can be characterized by its complex index of refraction which is taken to be constant with depth within the layer. Thus, this model can be used to represent homogeneous line structures with vertical edge walls. The spatial function representing the variation in the dielectric constant (square of the complex index of refraction) in the layer is expanded in a Fourier series. This series is substituted into the wave equation and the eigenvalue solutions to this equation which represent the waveguide modes are found. Assuming a single incident plane wave normal to the surface, the boundary value problem at the layer interfaces is solved to determine the Fourier coefficients in the expansions for the transmitted and reflected fields. This method allows the use of conventional scalar imaging theory to compute the image when no polarization effects are present. In such a case, the E- and H-field components are equivalent and either may be used in the scalar imaging equations.

To include the effects of partial coherence in the imaging system, it is possible to integrate over a finite illumination cone angle as long as the variation of the scattered field coefficients is negligible for the cone angle used. Hence, for layers approximately a few micrometers or less thick, finite coherence may be included.

This report covers the extension of this model by Kirk and Nyyssonen [6] to line structures of arbitrary edge geometry whose index of refraction may vary with depth in the layer. This line structure is approximated by subdividing it into a set of sublayers, each consisting of a line object with vertical edges and having a constant index of refraction over its small interval of depth. Each sublayer is treated in the same way as the single layer of Nyyssonen's earlier model. The waveguide modes and solution for the electromagnetic fields are found for each sublayer. There are now n+1 boundary value equations where n is the number of sublayers. These equations when solved allow for the substitution of a single "equivalent" planar scattering layer for the multilayer structure. Thereafter, the solution for the transmitted and reflected field components and image are found in the same manner as for the single layer case. This model therefore allows for the modeling of line structures which contain different materials, have curved edges, asymmetry, and unpatterned (or patterned) sublayers. The mathematical details of the model are given in the expanded version of ref. [6] reproduced in Appendix III. A list of definitions of symbols used in the software and Appendix III is given in the attached table.

Software Structure

As input to the software, the line structure may be characterized either by giving the index of refraction, thickness, and edge locations for the individual sublayers, or by a single refractive index, total thickness, and the polynomial coefficients used to

describe the edge geometry (See Appendix III.) In the latter case, the number of layers used to approximate this structure in the calculations must be designated. A good rule of thumb to use in determining the number of layers is to divide the change in linewidth (between the top and bottom interfaces) by 0.1 µm and use a value larger than this. For most cases of interest in integrated circuit processing, 9 layers are sufficient. The program arrays, as written, allow up to 20 layers. The program calculates both the scattered field and the microscope image for TE-mode illumination. That is, the direction of polarization (i.e. E-field) is assumed to be parallel to the length of the line structure.

The scattered field is given in terms of the Fourier coefficients of the resulting far field diffraction pattern. In the test cases shown, 45 coefficients are given corresponding to ± 22 diffracted orders at diffraction angles corresponding to $n\lambda/P$ where n is the order number, λ the wavelength, and P the period. The line structure is assumed to be repeated at a period P for convenience in calculating the Fourier series coefficients. An isolated line image is calculated by taking P large enough so that there is no influence from adjacent edges. Near resonances, this is not always possible due to time or storage limits on array sizes. The largest period used has been 12 µm corresponding to a 90x90 complex matrix for the boundary condition equations.

The microscopic image is calculated using conventional scalar imaging theory with the complex Fourier coefficients of the scattered field substituted for those of the planar object traditionally used. The software, as written, assumes a 1-D imaging system with a finite illumination cone angle. The Fourier coefficients of the scattered field are assumed to be constant over this angle. The calculations are accurate for a 2-D system as long as the condenser numerical aperture (N.A.) is much smaller

than that of the imaging objective. Hence, the calculations will accurately predict the image waveforms for the NBS laser system which has an objective N.A. of 0.85 or 0.95 and an illumination aperture 1/5 that of the objective at a wavelength of 514 nm.

The software also allows the calculation of the image for varying focus positions. Best focus is the top surface of the patterned layer. For all other focus positions, a quadratic phase factor is introduced (just as in scalar image theory).

The input for focus position is given as the number of wavelengths of defocus m where m is a dimensionless quantity. The relationship between the displacement of the measurement plane from the Gaussian focal plane, z, is given by

$$z = \frac{2}{\tan^2\theta} m$$

where λ is the wavelength and $\tan\theta$ is substituted for N.A. ($=\sin\theta$) for the high numerical apertures conventionally used for linewidth measurement.

Implementation and Testing

This software (See Appendix I) is written in ANSI FORTRAN 77 consisting of a main program and 9 modules. The software is portable except for the complex matrix subroutines used for calculation of the eigenvectors and eigenvalues and matrix inversions. The software requires highly accurate routines because of the cascading of matrix multiplications and inversions. Those used at NBS on the Cyber 855* are from the NAG library* [7]. If these

---

*Certain commercial equipment, instruments, or materials are identified in this paper in order to adequately specify experimental or computational procedure. Such identification does not imply recommendation or endorsement by the National Bureau of Standards, nor does it imply that the materials or equipment identified are necessarily the best available for the purpose.

routines are unavailable, the user may substitute others as noted in the software. However, several test conditions should be met. A symmetric line object should produce symmetric Fourier coefficients to at least six significant figures. Also, a single-layer, thick line object with complex index of refraction should produce the same image structure as for a single layer when divided into 20 sublayers (or the maximum number of sublayers to be used). Repeatability to three or four significant figures in the image is sufficient to ensure this. If the matrix routines are inaccurate, the errors will increase as the number of layers is increased. Test cases are given in Appendix II. These six test cases are designed to test different portions of the software. Successful execution of one test case does not guarantee accuracy for the others.

All of the data calculated are output to files for use with available graphics. Plotting routines are not included here because they tend to be system dependent and user requirements may vary.

Accuracy

Testing of this software poses a challenging problem in that the only cases for which answers are known do not fully test the algorithms. For example, in comparing this model with scalar theory, agreement can be expected only in the limit as the thickness of the patterned layer approaches zero. Test case #2 for a patterned 0.09 µm thick chromium layer is one such case which has been shown to agree with scalar theory. (See ref. 5.) Comparison has also been done for patterned thin layers of silicon dioxide showing excellent agreement. (See ref. 4.) In addition, it is required that the ratio of reflectivities of the patterned layer and substrate (or sublayers) away from the edges agrees with the values calculated from the Fresnel equations. (See ref. 8.) Otherwise, calculations can at this time only be compared with experimental measurements. This has been done for some cases

[6, 9]. However, although the agreement is good in most cases, the accuracy is suspect near resonances (where the line dimensions of width and/or thickness are equal to an integer multiple of the wavelength) and for small line dimensions. In both cases, the energy in the high spatial frequencies increases and errors in the eigenvalues and eigenvectors are expected to increase due to truncation errors.

Acknowledgments

A number of people have contributed to this software development. The original software was written for the Univac 1108 computer* by Chris Kirk while a research associate at NBS. The author wishes to especially thank Ruth Varner, NBS, for her assistance in converting this software for use on the Cyber 855.* The present software has been modified by the author to work for patterned metal layers. Other modifications to simplify its use and provide additional documentation have also been made.

References

1. D. Nyyssonen, "Calibration of Optical Systems for Linewidth Measurements on Wafers," Opt. Eng. 21, 882-887 (1982).

2. L. C. Martin, The Theory of the Microscope, (Blackie, London, 1966), Chapters V and VIII.

3. E. C. Kintner, "Method for the Calculation of Partially Coherent Imagery," Appl. Opt. 17, 2747-2753 (1978).

4. D. Nyyssonen, "Theory of Optical Edge Detection and Imaging of Thick Layers," J. Opt. Soc. Am. 72, 1425-1436 (1982).

---

*See previous footnote.

5. D. Nyyssonen, "Optical Linewidth Measurement on Patterned Metal Layers," Proc. SPIE Vol. 480, Integrated Circuit Metrology II, 65-70 (1984).

6. D. Nyyssonen and C. Kirk, "Modeling the Optical Microscope Images of Thick Layers for the Purpose of Linewidth Measurement," Proc. SPIE Vol. 538, Optical Microlithography IV, 179-187 (1985).

7. These routines are available from: Numerical Algorithms Group (NAG) Ltd., 7 Banbury Road, Oxford, Oxfordshire OX2 6NN, England.

8. D. Nyyssonen, "Narrow-Angle Laser Scanning Microscope System for Linewidth Measurement on Wafers," NBSIR (to be published).

9. C. Kirk, "A Study of the Instrumental Errors in Linewidth and Registration Measurements Made with an Optical Microscope," Presented at the SPIE 1987 Santa Clara Symposium on Microlithography, Vol. 775, Integrated Circuit Metrology, Inspection and Process Control.

Table: Definition of Symbols Used in Software

	Math Symbol	Software Label
Free space wavelength in microns	λ	WAVE
Total layer thickness	T	TL
The number of layers	N	NS
Period of the grating	P	PER
RI of the air layer	$\hat{n}_o$	CRI(0)
RI of the substrate	$\hat{n}_s$	CRI(21)
RI of the n-th layer	$\hat{n}_n$	CRI(N)
Width polynomial coefficients	X_j	W(J)
Starting points for 1st, 2nd, and 3rd order	Z_j	PO(J)
The X position offset for each layer	--	XP(J)
The Z locations of the layer interfaces	Z_n	ZP (N)
Spatial frequency of the grating	1/P	SPAFRE
Free space wavenumber (in units of μm^{-1})	k_o	RK0
Fourier coefficients of dielectric constant	$E_{q,n}$	EQ(I)
Eigenvalue matrix	$D_{i,j}$	D(I,J)
Eigenvalues of the layers	$\alpha_{m,n}$	VAL(M)
Eigenvectors of the layers	$B_{j,m,n}$	VEC
Boundary equation matrices	$D^{11}_{j,m}, D^{12}_{j,m}, D^{21}_{j,m}, D^{22}_{j,m}$	RM(L,M)
(A) coefficients	$A_{m,1}$, $A'_{m,1}$	AV(M)
Fourier coefficients of the pseudo-object	E^R_j	FC(J)
1-D image of the line	--	ELEC(I)

Appendix I
Computer Software Listing (THKIMAG)

```
 1          PROGRAM THKIMAG
 2 C
 3 C        THE ORIGINAL VERSION OF THIS PROGRAM WAS WRITTEN BY
 4 C        CHRIS KIRK, WHILE AN EMPLOYEE OF VICKERS INSTRUMENTS,
 5 C        (HAXBY ROAD, YORK, NORTH YORKSHIRE,ENGLAND) WHILE A
 6 C        RESEARCH ASSOCIATE AT THE NATIONAL BUREAU OF STANDARDS,
 7 C        GAITHERSBURG, MARYLAND, USA.  SEPTEMBER 1984.
 8 C
 9 C        THE CURRENT VERSION HAS BEEN MODIFIED BY D. NYYSSONEN
10 C        TO WORK FOR METAL LAYERS.  JUNE 1986
11 C
12 C        **********************************************************
13 C
14 C        THIS PROGRAM COMPUTES THE OPTICAL IMAGE OF LINE OBJECTS
15 C        WITH ARBITRARY EDGE GEOMETRY, PATTERNED IN THICK LAYERS
16 C        INCLUDING MULTILAYER STRUCTURES WITH SLOPING, CURVED, AND
17 C        UNDERCUT EDGES, AS WELL AS ASYMMETRIC OBJECTS.
18 C        SEE REFERENCE:  "MODELING OF THE OPTICAL IMAGING OF LINES
19 C        PATTERNED IN THICK LAYERS WITH VARIABLE EDGE GEOMETRY,"
20 C        BY D. NYYSSONEN AND C. P. KIRK
21 C        ALL EQUATION NUMBERS GIVEN REFER TO THIS MANUSCRIPT
22 C        FOR QUESTIONS CONCERNING THIS PROGRAM CONTACT:
23 C        R. D. LARRABEE, PRECISION ENGINEERING DIVISION, NATIONAL
24 C        BUREAU OF STANDARDS OR D. NYYSSONEN, CD METROLOGY, INC.
25 C
26 C        ***********************************************************
27 C
28 C        SYSTEM DEPENDENT FEATURES.
29 C        ----------------------------------------------------------
30 C
31 C        ALTHOUGH THIS SOFTWARE HAS BEEN WRITTEN IN FORTRAN 77 IN
32 C        ORDER TO ALLOW FOR EASY PORTABILITY, THERE ARE A NUMBER
33 C        OF FEATURES WHICH MAY BE SYSTEM DEPENDENT.
34 C
35 C        1.   A FORTRAN 77 COMPILER IS REQUIRED.
36 C        2.   THE SYSTEM MUST SUPPORT CERTAIN NAG LIBRARY ROUTINES.
37 C
38 C        A NOTE CONCERNING THE NAG LIBRARY.
39 C        ----------------------------------------------------------
40 C
41 C        THIS PROGRAM USES THE FOLLOWING NAG ROUTINES.
42 C
43 C        F02AKF      F04ADF
44 C
45 C        THESE ARE SINGLE PRECISION VERSIONS OF LIBRARY ROUTINES
46 C        FOR THE CYBER WHICH MAY NOT BE SUPPORTED ON ALL
47 C        MACHINES.
48 C
49 C        THESE ROUTINES ARE AVAILABLE FROM:
50 C
```

```
 51 C         NUMERICAL ALGORITHMS GROUP (NAG) LTD, 7 BANBURY ROAD,
 52 C         OXFORD, OXFORDSHIRE. OX2 6NN. ENGLAND.
 53 C
 54 C         **********************************************************
 55           PARAMETER (NLAY=20, NLAY1=21)
 56           PARAMETER(NLIM=-22, LIM=22, KLIM=45, MLIM=90)
 57           REAL PI,RK0,WAVE,SPAFRE,WI(NLAY),ZP(0:NLAY),NS,XP(NLAY),TRA(2)
 58           COMPLEX D(NLIM:LIM,NLIM:LIM),RM(MLIM,MLIM),T(MLIM,MLIM)
 59      *    ,RN(KLIM,MLIM),AV(MLIM),FC(NLIM:LIM),CRI(0:NLAY1),Q0,VAL(KLIM)
 60           PI = 4.0*ATAN(1.0)
 61           OPEN (UNIT=9,FILE='PARFIL')
 62           OPEN (UNIT=10,FILE='FCOFDC')
 63           OPEN (UNIT=11,FILE='DMATRX')
 64           OPEN (UNIT=12,FILE='EIGVAL')
 65           OPEN (UNIT=13,FILE='EIGVEC')
 66           OPEN (UNIT=14,FILE='BOUNEQ')
 67           OPEN (UNIT=15,FILE='BEMATX')
 68           OPEN (UNIT=16,FILE='FCOFPO')
 69           OPEN (UNIT=17,FILE='IMAGE')
 70 C
 71 C         **********************************************************
 72 C
 73 C         SUMMARY OF THE INPUT/OUTPUT STRUCTURE.
 74 C         ----------------------------------------------------------
 75 C
 76 C         INPUT                        INPUT DATA FILE.
 77 C         PARFIL       UNIT9           PARAMETER FILE CREATED.
 78 C         FCOFDC       UNIT10          FOURIER COEFFICIENTS OF
 79 C                                      DIELECTRIC CONSTANT CALCULATED
 80 C                                      FOR FIRST LAYER.
 81 C         DMATRX       UNIT11          EIGENVALUE MATRIX D OF THE 1ST
 82 C                                      LAYER.
 83 C         EIGVAL       UNIT12          EIGENVALUES OF THE LAYERS.
 84 C         EIGVEC       UNIT13          EIGENVECTORS OF THE LAYERS.
 85 C         BOUNEQ       UNIT14          BOUNDARY EQUATION MATRICES.
 86 C         BEMATX       UNIT15          (A) COEFFICIENTS.
 87 C         FCOFPO       UNIT16          FOURIER COEFFICIENTS OF
 88 C                                      THE PSEUDO-OBJECT.
 89 C         IMAGE        UNIT17          1-D IMAGE OF THE LINE.
 90 C
 91 C         **********************************************************
 92 C
 93 C         SET UP THE  PARAMETERS FOR THE SECTIONED LINE.
 94 C         ----------------------------------------------------------
 95 C
 96 C         INPUT
 97 C            WAVE   = FREE SPACE WAVELENGTH IN MICRONS.
 98 C            NS     = THE NUMBER OF LAYERS.
 99 C            PER    = THE PERIOD.
100 C            CRI(0) = RI OF THE AIR LAYER.
```

```
101 C            CRI(21)= RI OF THE SUBSTRATE.
102 C            ID     = DEFINE LINE:  PARAMETRICALLY(0)
103 C                   =             :  LAYER BY LAYER(1).
104 C            W(I)   = WIDTH POLYNOMIAL COEFFICIENTS.  I=ORDER
105 C            PO(I)  = STARTING POINTS FOR 1ST, 2ND AND 3RD ORDER.
106 C            CRI(1) = REFRACTIVE INDEX OF PATTERNED LAYER.
107 C            TL     = LAYER THICKNESS.
108 C            TRA(1) = PHOTOMULTIPLIER SLIT WIDTH.
109 C            TRA(2) = TELEVISION CAMERA GAUSSIAN WIDTH PARAMETER.
110 C            LSKIP  = 0:  GENERATE A NEW FOURIER SERIES FOR
111 C                            THE PSEUDO OBJECT.
112 C                     1:  USE PREVIOUSLY GENERATED FOURIER SERIES.
113 C                    -1:  GENERATE THE IMAGE.
114 C            DF = DEFOCUS IN WAVES WHERE DF IS A DIMENSIONLESS QUANTITY.
115 C            IF DEFOCUS IS KNOWN IN TERMS OF DISPLACEMENT OF THE
116 C            MEASUREMENT PLANE FROM THE FOCAL PLANE DZ, IT MUST BE
117 C            CONVERTED TO WAVES USING THE RELATIONSHIP:
118 C               DZ=(2*WAVE/(TAN(ANGLE))**2)*DF
119 C            WHERE ANGLE IS THE SAME AS DEFINED BY N.A. = SIN(ANGLE)
120 C            INPUT IF ID = 1.
121 C               WI(N)    = THE WIDTH OF THE LINES IN THE NTH LAYER.
122 C               ZP(N)    = THE Z LOCATIONS OF THE LAYER INTERFACES.
123 C               CRI(N)   = RI OF EACH LAYER.
124 C               XP(N)    = THE X POSITION OFFSET FOR EACH LAYER.
125 C
126 C            COMPUTATION
127 C               SPAFRE   = SPATIAL FREQUENCY OF THE GRATING (1/PERIOD).
128 C
129 C            COMPUTATIONS IF ID = 0.
130 C               CRI(N)   = RI OF EACH LAYER.
131 C               WI(N)    = THE WIDTHS OF THE LINES IN EACH LAYER.
132 C               ZP(N)    = THE Z LOCATIONS OF THE LAYER INTERFACES.
133 C                          THE TOP SURFACE IS ASSUMED TO BE Z=0.
134 C               XP(N)    = THE X POSITION OFFSET FOR EACH LAYER (FOR
135 C                          ASYMMETRIC CROSS-SECTIONS).
136 C
137 C            COMPUTATION
138 C               RK0 = FREE SPACE WAVENUMBER (IN UNITS OF 1/UM).
139 C
140          CALL LINE(PI,WAVE,RK0,CRI,ZP,WI,NS,SPAFRE,
141       *  TRA,XP,DF,LSKIP)
142 C
143 C        NOTE: CALCULATIONS ARE FOR LINE OBJECT, SPACES ARE
144 C        CALCULATED BY TAKING LINEWIDTH = PERIOD MINUS
145 C        DESIRED SPACE WIDTH.
146 C
147 C        ***********************************************************
148 C
149 C        IF LSKIP =1 THEN GO STRAIGHT TO THE IMAGE SUBROUTINE.
150 C
```

```
151              IF (LSKIP.EQ.1) GO TO 20
152 C
153 C            ***********************************************************
154 C
155 C            FIND THE EIGENVALUES AND EIGENVECTORS FOR EACH LAYER.
156 C
157 C            D IS THE EIGENVALUE MATRIX FOR EACH LAYER.
158 C            THE EIGENVALUES AND EIGENVECTORS ARE FOUND FOR EACH LAYER
159 C            AND THEN STORED ON DISK, STARTING WITH THE TOP LAYER.
160 C
161 C            THE DIFFRACTION SERIES IS TRUNCATED FOR DIFFRACTION
162 C            ANGLES WHICH EXCEED 90 DEGREES IN AIR.  THIS IS SET
163 C            BY THE VARIABLE 'LIM'.  LIM AND ITS RELATED VARIABLES
164 C            ARE SET IN THE PARAMETER STATEMENTS.
165 C
166 C            L = (REFRACTIVE INDEX OF AIR)*(PERIOD)/(WAVELENGTH)
167 C            NLIM = -L, LIM = L, KLIM = 2L+1, MLIM = 2(2L+1)
168 C
169              DO 10 N=1,NS
170                CALL SETUPD(PI,WI(N),CRI,D,SPAFRE,N,XP(N),WAVE,Q0,EQ2)
171                CALL EIGD(D,N,Q0,RK0,WAVE,SPAFRE,EQ2)
172   10         CONTINUE
173 C
174 C            ***********************************************************
175 C
176 C            SET UP THE MATRIX ELEMENTS FOR THE FIRST INTERFACE
177 C            BOUNDARY CONDITIONS.
178 C            -----------------------------------------------------------
179 C
180 C            THE ARRAY RM CONTAINS THE UPPER MATRIX ELEMENTS (SEE EQ. 21).
181 C
182              CALL SETRM(RM,RK0,WAVE,SPAFRE,CRI(0))
183 C
184 C            ***********************************************************
185 C
186 C            SET UP THE PRODUCT MATRICES FOR THE N-LAYERS INTERFACES
187 C            -----------------------------------------------------------
188 C
189 C            SET THE MATRIX T TO THE IDENTITY MATRIX.
190 C            THE T MATRIX IS MODIFIED BY ALL THE INTERMEDIATE INTERFACES.
191 C            STARTING WITH THE IDENTITY MATRIX, THE T MATRIX IS PASSED
192 C            TO THE SUBROUTINE FOR EACH INTERFACE AND RETURNED AFTER
193 C            MODIFICATION.
194 C
195              DO 40 L=1,MLIM
196                DO 30 M=1,MLIM
197                  IF(L.EQ.M) THEN
198                    T(L,M) = CMPLX(1.0,0.0)
199                  ELSE
200                    T(L,M) = CMPLX(0.0,0.0)
```

```
201                END IF
202   30         CONTINUE
203   40       CONTINUE
204            IF(NS.GT.1) THEN
205              DO 50 N=1,NS-1
206                CALL SETPQN(N,ZP(N),T)
207   50         CONTINUE
208            END IF
209 C
210 C          ***********************************************************
211 C
212 C          SET UP THE MATRIX ELEMENTS FOR THE LAST INTERFACE BOUNDARY
213 C          CONDITIONS.
214 C          -----------------------------------------------------------
215 C
216 C          THE ARRAY RN CONTAINS THE LAST INTERFACE MATRIX
217 C          ELEMENTS.
218 C
219            CALL SETRN(RN,NS,ZP(NS),VAL)
220 C
221 C          SOLVE THE MATRIX EQUATION FOR THE (A) COEFFICIENTS.  (EQ. 21)
222 C
223 C          THE VECTOR AV IS RETURNED CONTAINING THE (A) COEFFICIENTS.
224 C
225            CALL SETAM(RM,T,RN,RK0,AV,VAL,NS,WAVE,SPAFRE,CRI(21))
226 C
227 C          SET UP THE FOURIER COEFFICIENTS.
228 C          -----------------------------------------------------------
229 C
230 C          THE FOURIER COEFFICIENTS ARE RETURNED IN VECTOR FC.
231 C          T IS USED AS A WORKSPACE.
232 C
233            CALL FCOEFF(AV,FC,T)
234   20       CONTINUE
235 C
236 C          IF LSKIP = -1 THEN SKIP THE IMAGE ROUTINE.
237 C
238            IF (LSKIP.EQ.-1) GOTO 60
239 C
240 C          COMPUTE THE IMAGE FROM THE FOURIER COEFFICIENTS.
241 C          -----------------------------------------------------------
242 C
243            CALL IMAGE(FC,PI,SPAFRE,TRA,DF,LSKIP,WAVE)
244 C
245   60       CONTINUE
246            STOP
247           END
248 C
249 C          ***********************************************************
250 C          ***********************************************************
```

```
251 C
252 C         SUBROUTINES TO SUPPORT THE MAIN PROGRAM.
253 C
254 C         **************************************************************
255 C
256           SUBROUTINE LINE(PI,WAVE,RK0,CRI,ZP,WI,NS,SPAFRE,
257      *    TRA,XP,DF,LSKIP)
258           COMPLEX CRI(0:21)
259           REAL PI,RK0,WAVE,SPAFRE,W(0:3),WI(20),PER,PO(3),
260      *      Z,ZP(0:20),NS,TL,XP(20),TRA(2)
261 C
262 C         SET THE ARRAYS TO ZERO.
263 C
264           DO 210 I=0,20
265             ZP(I) = 0.0
266             CRI(I) = CMPLX(0.0,0.0)
267             IF(I.GT.0) THEN
268               WI(I) = 0.0
269               XP(I) = 0.0
270             END IF
271  210      CONTINUE
272 C
273 C         READ IN THE WAVELENGTH, THE PERIOD, THE NUMBER OF LAYERS
274 C
275           READ*,WAVE,PER,NS
276           SPAFRE = 1.0/PER
277 C
278 C         READ IN THE RI'S OF THE AIR LAYER AND THE SUBSTRATE.
279 C         ID DETERMINES WHETHER THE LINE IS DEFINED BY PARAMETERS
280 C         OR LAYER BY LAYER.
281 C
282           READ*,CRI(0),CRI(21),ID
283 C
284 C         READ IN THE WIDTH POLYNOMIAL COEFFICIENTS.
285 C
286           READ*,W(0),W(1),W(2),W(3)
287 C
288 C         READ IN THE Z POSITION STARTING POINTS FOR THE 1ST,2ND
289 C         AND 3RD ORDERS.
290 C
291           READ*,PO(1),PO(2),PO(3)
292 C
293 C         READ IN THE REFRACTIVE INDEX OF THE PATTERNED LAYER
294 C         AND THE LAYER THICKNESS.
295 C
296           READ*,CRI(1),TL
297 C
298 C         READ IN THE PHOTOMULTIPLIER SLIT WIDTH AND THE VIDEO
299 C         CAMERA WIDTH PARAMETER.
300 C
```

```
301               READ*,TRA(1),TRA(2)
302               IF(TRA(1).GT.0.01) THEN
303                 TRA(2) = 0.0
304               END IF
305 C
306 C             THE CAMERA WIDTH PARAMETER TRA(2) IS SET TO ZERO WHENEVER
307 C             THERE IS A FINITE SLIT WIDTH TRA(1).
308 C
309 C
310 C             READ IN THE SKIP PARAMETER (TO SKIP IMAGE CALCULATIONS)
311 C             AND THE AMOUNT OF DEFOCUS IN NUMBER OF WAVES.
312 C
313 C
314               READ*,LSKIP,DF
315 C
316               IF(ID.EQ.0) THEN
317 C
318 C               SET UP THE LINE DEFINED PARAMETRICALLY.
319 C
320                 DO 220 I=1,NS
321                   CRI(I) = CRI(1)
322                   Z = TL*(I-0.5)/NS
323                   WI(I) = W(3)*(Z-PO(3))**3+W(2)*(Z-PO(2))**2
324                   WI(I) = WI(I)+W(1)*(Z-PO(1))+W(0)
325                   ZP(I) = TL*I/NS
326  220            CONTINUE
327               ELSE IF(ID.EQ.1) THEN
328 C
329 C               SET UP THE LINE LAYER BY LAYER.
330 C
331 C               READ IN THE WIDTH, INTERFACE POSITION RI, AND X OFFSET
332 C               OF EACH LAYER
333 C
334                 DO 230 I=1,NS
335                   READ*,WI(I),ZP(I),CRI(I),XP(I)
336 230             CONTINUE
337               END IF
338 C
339 C             CALCULATE THE WAVE NUMBER.
340 C
341               RK0 = 2.0*PI/WAVE
342
343 C             SEND PARAMETERS TO A FILE.
344 C
345               WRITE(9,*) 'RUN PARAMETERS.'
346               WRITE(9,*) 'WAVELENGTH = ',WAVE
347               WRITE(9,*) 'NUMBER OF LAYERS=',NS
348               WRITE(9,*) 'WAVE NUMBER =',RK0
349               WRITE(9,*) 'AIR LAYER =',CRI(0)
350               WRITE(9,*) 'SUBSTRATE =',CRI(21)
```

```
351           WRITE(9,*) 'DEFOCUS =',DF
352           WRITE(9,*) 'SLIT WIDTH IN MICRONS =',TRA(1)
353           WRITE(9,*) 'CAMERA WIDTH PARAMETER =',TRA(2)
354           IF(LSKIP.LE.0) THEN
355           WRITE(9,*) 'LAYER     WIDTH     POSITION      RI       OFFSET'
356             DO 299 I=1,NS
357               WRITE(9,240) I,WI(I),ZP(I),CRI(I),XP(I)
358   240         FORMAT (1X,I2,6X,F6.3,6X,F5.3,4X,F5.3,1X,F5.3,
359      *        6X,F5.3)
360   299       CONTINUE
361           END IF
362           RETURN
363           END
364 C
365 C         **********************************************************
366 C
367           SUBROUTINE SETUPD(PI,W,CRI,D,SPAFRE,N,XP,WAVE,Q0)
368           PARAMETER(NLIM=-22, LIM=22, KLIM=45, MLIM=90)
369           REAL PI,G05CAF,SPAFRE,RP,W,XP,RIP,WAVE
370           COMPLEX D(NLIM:LIM,NLIM:LIM),EQ(NLIM:LIM),E1,CI,Q0,
371      *      CRI(0:21)
372 C
373 C         W = LINEWIDTH OF LAYER N.
374 C         XP = X OFFSET OF THE LINE IN LAYER N.
375 C
376 C         THE LAYER FOURIER COEFFICENTS FOR THE EXPANSION OF THE
377 C         DIELECTRIC CONSTANT ARE STORED IN ARRAY EQ.
378           CI = CMPLX(0.0,1.0)
379 C
380 C
381 C         SET THE ARRAYS TO ZERO.
382 C
383           DO 320 I=NLIM,LIM
384             EQ(I) = CMPLX(0.0,0.0)
385             DO 310 J=NLIM,LIM
386               D(I,J) = CMPLX(0.0,0.0)
387   310       CONTINUE
388   320     CONTINUE
389 C
390 C         ROUTINE TO GENERATE THE FOURIER COEFFICIENTS.
391 C         THE OFFSET XP ADDS A PHASE TERM TO THE FOURIER
392 C         COEFFICIENTS.  SEE EQUATION 8 OF APPENDIX III.
393 C
394           E1 = CRI(N)**2 - CRI(0)**2
395           EQ(0) = CRI(0)**2+E1*W*SPAFRE
396           DO 330 I=NLIM,LIM
397             IF(I.EQ.0) GO TO 330
398               EQ(I) = E1*SIN(PI*I*SPAFRE*W)/PI/I
399               EQ(I) = EQ(I)*CEXP(2.0*PI*CI*SPAFRE*XP*I)
400             IF(N.EQ.1) THEN
```

```
401                 WRITE(10,*) EQ(I),I
402               END IF
403  330        CONTINUE
404               Q0 = EQ(0)
405 C
406 C           ROUTINE TO CONSTRUCT THE D MATRIX.  SEE APPENDIX OF
407 C              APPENDIX III.
408             DO 350 L=NLIM,LIM
409               DO 340 M=NLIM,LIM
410                 IF(L.EQ.M) THEN
411                   D(L,M) = -(WAVE*L*SPAFRE)**2
412                 ELSE IF((IABS(L-M)).GT.22)THEN
413                   D(L,M) = CMPLX(0.0,0.0)
414                 ELSE
415                   D(L,M) = EQ(M-L)
416                 END IF
417  340          CONTINUE
418  350        CONTINUE
419             RETURN
420             END
421 C
422 C           ***********************************************************
423 C
424             SUBROUTINE EIGD(D,N,Q0,RK0)
425             PARAMETER(NLIM=-22, LIM=22, KLIM=45, MLIM=90  )
426             COMPLEX D(KLIM,KLIM),VAL(KLIM),Q0
427             REAL AR(KLIM,KLIM),AI(KLIM,KLIM),RR(KLIM),
428        *    RI(KLIM),VR(KLIM,KLIM),VI(KLIM,KLIM),IWORK(KLIM),RK0
429 C
430 C           THE D MATRIX FOR THE FIRST LAYER IS WRITTEN ON TAPE11.
431 C           THE COMPLEX D MATRIX IS SPLIT INTO TWO REAL MATRICES
432 C           AND STORED IN ARRAYS AR() (REAL) AND AI() (IMAGINARY).
433 C
434             DO 420 I=1,KLIM
435               RR(I) = 0.0
436               RI(I) = 0.0
437               IWORK(I) = 0.0
438               DO 410 J=1,KLIM
439                 VR(I,J) = 0.0
440                 VI(I,J) = 0.0
441                 AR(I,J) = REAL(D(I,J))
442                 IF(ABS(AR(I,J)).LT.1.E-9) AR(I,J)=+0.0
443                 AI(I,J) =AIMAG(D(I,J))
444                 IF(ABS(AI(I,J)).LT.1.E-9) AI(I,J)=+0.0
445                 IF(N.EQ.1) THEN
446                   WRITE(11,*) D(I,J),I,J
447                 END IF
448  410          CONTINUE
449  420        CONTINUE
450 C
```

```
451 C          F02AKF SOLVES FOR THE EIGENVALUES AND EIGENVECTORS.
452 C          THE VECTORS ARE RETURNED IN VR AND VI AND THE EIGENVALUES
453 C          ARE RETURNED IN RR AND RI.
454 C          THE SQUARE ROOTS OF THE EIGENVALUES ARE WRITTEN ON
455 C          TAPE12 AND THE EIGENVECTORS ON TAPE13.
456 C
457            IFAIL = 0
458            CALL F02AKF(AR,KLIM,AI,KLIM,KLIM,RR,RI,VR,KLIM,VI,KLIM,
459       *    IWORK,IFAIL)
460 C
461 C          THE CYBER RESTRICTS PHASE ANGLES ON SQRT OF A COMPLEX
462 C          NO. TO -PI/2<0<PI/2 WHICH RESULTS IN INCORRECT
463 C          PHASE ANGLES.  ANGLES ARE CORRECTED FOLLOWING
464 C          CALCULATION OF CSQRT.
465 C
466            DO 440 I=1,KLIM
467              VAL(I) = CMPLX(RR(I),RI(I))
468              VAL(I) = -VAL(I)-Q0
469              VAL(I) = CSQRT(VAL(I))*RK0
470              IF(AIMAG(VAL(I)).LT.0.0) THEN
471                VAL(I) = -VAL(I)
472              END IF
473              WRITE(12,*) VAL(I)
474              PRINT*,VAL(I),I
475              DO 430 J=1,KLIM
476                WRITE(13,*) VR(I,J),VI(I,J)
477  430         CONTINUE
478  440       CONTINUE
479            IF(IFAIL.EQ.0) THEN
480              PRINT*,'EIGENVALUE SUCCESS AT LAYER',N
481            ELSE
482              PRINT*,'EIGENVALUE FAILURE AT LAYER',N
483            END IF
484            RETURN
485            END
486 C
487 C          **********************************************************
488 C
489            SUBROUTINE SETRM(RM,RK0,WAVE,SPAFRE,CR0)
490            PARAMETER(NLIM=-22, LIM=22, KLIM=45, MLIM=90)
491            COMPLEX RM(MLIM,MLIM),VEC,VECCN,VAL(KLIM),CI,RKL,V,CR0
492            REAL VR,VI,RK0,WAVE,SPAFRE
493 C
494 C          CR0 = REFRACTIVE INDEX OF THE AIR LAYER.
495 C
496 C          THE EIGENVALUE AND EIGENVECTORS ARE RECOVERED FOR THE
497 C          FIRST LAYER FROM UNIT12 AND UNIT13.
498 C
499            REWIND 12
500            REWIND 13
```

```
501           CI = CMPLX(0.0,-1.0)
502           DO 520 L=1,KLIM
503             V = CMPLX((WAVE*SPAFRE*(L-LIM-1))**2,0.0)
504             RKL = CSQRT(CR0**2-V)
505             DO 510 M=1,KLIM
506               IF(L.EQ.1) THEN
507                 READ(12,*) VAL(M)
508               END IF
509               READ(13,*) VR,VI
510               VEC = CMPLX(VR,VI)
511               RM(L,M) = (RKL-VAL(M)*CI/RK0)*VEC
512               RM(L,M+KLIM) = (RKL+VAL(M)*CI/RK0)*VEC
513               RM(L+KLIM,M) = CMPLX(0.0,0.0)
514               RM(L+KLIM,M+KLIM) = CMPLX(0.0,0.0)
515  510        CONTINUE
516  520      CONTINUE
517           RETURN
518           END
519 C
520 C         ***********************************************************
521 C
522           SUBROUTINE SETPQN(N,ZP1,T)
523           PARAMETER(NLIM=-22, LIM=22, KLIM=45, MLIM=90)
524           COMPLEX PQ(MLIM,MLIM),T(MLIM,MLIM),RIPQ(MLIM,MLIM),
525      *    VEC,VECCN,VAL(KLIM)
526           REAL WKSPCE(MLIM),ZP1,VR,VI
527 C
528 C         ZP1 = THE Z LOCATION OF THE INTERFACE.
529 C
530           REWIND 12
531           REWIND 13
532 C
533 C         READ PAST THE EIGENVALUES AND EIGENVECTORS RELATING TO
534 C         THE PREVIOUS LAYERS.
535 C
536           IF(N.GT.1) THEN
537             DO 630 I=1,N-1
538               DO 620 J=1,KLIM
539                 READ(12,*) VAL(J)
540                 DO 610 K=1,KLIM
541                   READ(13,*) VR,VI
542  610            CONTINUE
543  620          CONTINUE
544  630        CONTINUE
545           END IF
546 C
547 C         SET UP THE UPPER LAYER MATRIX.
548 C
549           DO 650 L=1,KLIM
550             DO 640 M=1,KLIM
```

```
551                  IF(L.EQ.1) THEN
552                    READ(12,*) VAL(M)
553                  END IF
554                  READ(13,*) VR,VI
555                  VEC = CMPLX(VR,VI)
556                  PQ(L,M) = VEC*CEXP(-VAL(M)*ZP1)
557                  PQ(L,M+KLIM) = VEC*CEXP(VAL(M)*ZP1)
558                  PQ(L+KLIM,M) = VAL(M)*PQ(L,M)
559                  PQ(L+KLIM,M+KLIM) = -VAL(M)*PQ(L,M+KLIM)
560   640          CONTINUE
561   650        CONTINUE
562 C
563 C            MULTIPLY THE PREVIOUS T MATRIX BY THE UPPER LAYER MATRIX.
564 C
565              DO 685 L=1,MLIM
566                DO 680 M=1,MLIM
567                  RIPQ(L,M) = CMPLX(0.0,0.0)
568                  DO 675 I=1,MLIM
569                    RIPQ(L,M) = RIPQ(L,M)+PQ(L,I)*T(I,M)
570   675            CONTINUE
571   680          CONTINUE
572   685        CONTINUE
573 C
574 C            WRITE THE MATRIX PRODUCT ONTO UNIT14.
575 C            CLEAR THE MATRICES RIPQ AND T.
576 C
577              REWIND 14
578              DO 658 L=1,MLIM
579                DO 654 M=1,MLIM
580                  WRITE(14,*) RIPQ(L,M)
581                  RIPQ(L,M) = CMPLX(0.0,0.0)
582                  IF(L.EQ.M) THEN
583                    T(L,M) = CMPLX(1.0,0.0)
584                  ELSE
585                    T(L,M) = CMPLX(0.0,0.0)
586                  END IF
587   654          CONTINUE
588   658        CONTINUE
589 C
590 C            SET UP THE LOWER LAYER MATRIX.
591 C
592              DO 670 L=1,KLIM
593                DO 660 M=1,KLIM
594                  IF(L.EQ.1) THEN
595                    READ(12,*) VAL(M)
596                  END IF
597                  READ(13,*) VR,VI
598                  VEC = CMPLX(VR,VI)
599                  PQ(L,M) = VEC*CEXP(-VAL(M)*ZP1)
600                  PQ(L,M+KLIM) = VEC*CEXP(VAL(M)*ZP1)
```

```
601                 PQ(L+KLIM,M) = VAL(M)*PQ(L,M)
602                 PQ(L+KLIM,M+KLIM) = -VAL(M)*PQ(L,M+KLIM)
603  660          CONTINUE
604  670        CONTINUE
605 C
606 C           F04ADF INVERTS THE MATRIX PQ AND RETURNS THE INVERSE IN
607 C           THE MATRIX RIPQ.
608 C
609             IFAIL = 0
610             CALL F04ADF(PQ,MLIM,T,MLIM,MLIM,MLIM,RIPQ,MLIM,
611        *    WKSPCE,IFAIL)
612             IF(IFAIL.EQ.0) THEN
613               PRINT*,'SUCCESSFUL MATRIX INVERSION AT INTERFACE',N
614             ELSE
615               PRINT*,'SINGULAR MATRIX AT INTERFACE',N
616             STOP
617             END IF
618 C
619 C           RECOVER THE PREVIOUS MATRIX FROM UNIT14.
620 C
621             REWIND 14
622             DO 608 L=1,MLIM
623               DO 604 M=1,MLIM
624                 READ(14,*) PQ(L,M)
625  604          CONTINUE
626  608        CONTINUE
627 C
628 C           MULTIPLY THE TWO MATRICES AND RETURN THE PRODUCT IN T.
629 C
630             DO 694 L=1,MLIM
631               DO 694 M=1,MLIM
632                 T(L,M) = CMPLX(0.0,0.0)
633                 DO 690 I=1,MLIM
634                   T(L,M) = T(L,M)+RIPQ(L,I)*PQ(I,M)
635  690            CONTINUE
636  694          CONTINUE
637  698        CONTINUE
638             RETURN
639             END
640 C
641 C           ***********************************************************
642 C
643             SUBROUTINE SETRN(RN,NS,ZS,VAL)
644             PARAMETER (NLIM=-22, LIM=22, KLIM=45, MLIM=90)
645             COMPLEX RN(KLIM,MLIM),VEC,VECCN,VAL(KLIM)
646             REAL VR,VI,ZS,NS
647 C
648 C           ZS = THE Z POSITION OF THE SUBSTRATE INTERFACE.
649 C           CRS = THE COMPLEX REFRACTIVE INDEX OF THE SUBSTRATE.
650 C
```

```
651           REWIND 12
652           REWIND 13
653 C
654 C         SKIP OVER THE ALPHA(M) AND B(L,M) TERMS OF THE UPPER
655 C         LAYERS.
656 C
657           IF(NS.GT.1) THEN
658             DO 730 I=1,NS-1
659               DO 720 J=1,KLIM
660                 READ(12,*) VAL(J)
661                 DO 710 K=1,KLIM
662                   READ(13,*) VR,VI
663  710            CONTINUE
664  720          CONTINUE
665  730        CONTINUE
666           END IF
667 C
668 C         SET UP THE RN MATRIX.
669           DO 750 L=1,KLIM
670             DO 740 M=1,KLIM
671               IF(L.EQ.1)  THEN
672                 READ(12,*) VAL(M)
673               END IF
674               READ(13,*) VR,VI
675               VEC = CMPLX(VR,VI)
676               RN(L,M)= CEXP(-VAL(M)*ZS)*VEC
677               RN(L,M+KLIM) = CEXP(VAL(M)*ZS)*VEC
678  740        CONTINUE
679  750      CONTINUE
680           RETURN
681           END
682 C
683 C         ***********************************************************
684 C
685           SUBROUTINE SETAM(RM,T,RN,RK0,AV,VAL,NS,WAVE,SPAFRE,CRS)
686           PARAMETER(NLIM=-22, LIM=22, KLIM=45, MLIM=90)
687           COMPLEX RM(MLIM,MLIM),T(MLIM,MLIM),RN(KLIM,MLIM),RKL,
688      *    RV(MLIM),AV(MLIM),CI,VAL(KLIM),CRS,CRSUB,S2,S3,A1,ASUB
689           REAL RK0,WKSPCE(MLIM),WAVE,SPAFRE,NS
690 C
691 C         ASSEMBLE THE RM,RN AND T MATRICES INTO ONE MATRIX (RM).
692 C
693 C     THIS VERSION ALLOWS FOR THE INCLUSION OF AN UNPATTERNED
694 C     SUBLAYER (OXIDE).  IF NOT WANTED, SET TSUB=0.0
695 C     TSUB IS THE THICKNESS IN UM OF THIS LAYER AND CRSUB IS
696 C     THE COMPLEX INDEX OF REFRACTION.
697 C
698           TSUB = 0.0
699           CRSUB = CMPLX(1.46,0.0)
700           CI = CMPLX(0.0,-1.0)
```

```
701              IF(NS.EQ.1) THEN
702              DO 820 L=1,KLIM
703                V = CMPLX((WAVE*SPAFRE*(L-LIM-1))**2,0.0)
704                S2 = CSQRT(CRSUB**2-V)
705                S3 = CSQRT(CRS**2-V)
706                A1 = CEXP(CMPLX(0.0,2.0)*RK0*TSUB*S2)
707                ASUB = ((S2+S3)-(S2-S3)*A1)/((S2+S3)+(S2-S3)*A1)
708                RKL = ASUB*S2
709                DO 810 M=1,KLIM
710                    RM(L+KLIM,M) = RN(L,M)*(RKL+VAL(M)*CI/RK0)
711                    RM(L+KLIM,M+KLIM) = RN(L,M+KLIM)*(RKL-VAL(M)*CI/RK0)
712   810          CONTINUE
713   820        CONTINUE
714            ELSE
715             DO 836 L=1,KLIM
716                V = CMPLX((WAVE*SPAFRE*(L-LIM-1))**2,0.0)
717                S2 = CSQRT(CRSUB**2-V)
718                S3 = CSQRT(CRS**2-V)
719                A1 = CEXP(CMPLX(0.0,2.0)*RK0*TSUB*S2)
720                ASUB = ((S2+S3)-(S2-S3)*A1)/((S2+S3)+(S2-S3)*A1)
721                RKL = ASUB*S2
722                DO 834 M=1,KLIM
723                  DO 832 I=1,KLIM
724                  RM(L+KLIM,M) = RM(L+KLIM,M) + RKL*(RN(L,I)*T(I,M) +
725       *          RN(L,I+KLIM)*T(I+KLIM,M)) + (RN(L,I)*VAL(I)*CI/RK0*
726       *          T(I,M) - RN(L,I+KLIM)*VAL(I)*CI/RK0*T(I+KLIM,M))
727                  RM(L+KLIM,M+KLIM) = RM(L+KLIM,M+KLIM) + RKL*(RN(L,I)*
728       *          T(I,M+KLIM) + RN(L,I+KLIM)*T(I+KLIM,M+KLIM)) +
729       *          (RN(L,I)*VAL(I)*CI/RK0*T(I,M+KLIM) - RN(L,I+KLIM)*
730       *          VAL(I)*CI/RK0*T(I+KLIM,M+KLIM))
731    832           CONTINUE
732    834         CONTINUE
733    836       CONTINUE
734            END IF
735 C
736 C            SET UP THE RIGHT HAND SIDE VECTOR RV.
737 C
738              DO 840 L=1,MLIM
739                WKSPCE(L) = 0.0
740                RV(L) = CMPLX(0.0,0.0)
741   840        CONTINUE
742             RV(LIM+1)=CMPLX(2.0,0.0)
743 C
744 C            F04ADF SOLVES THE SET OF SIMULTANEOUS EQUATIONS DEFINED
745 C            BY RM AND RV.  SEE EQ. 21 OF APPENDIX III.
746 C            THE SOLUTIONS ARE RETURNED IN THE VECTOR AV.
747 C
748              IFAIL = 0
749 C
750                PRINT *, '4 SECTIONS OF RM MATRIX'
```

```
751 C
752             WRITE(1,*)'FIRST SECTION RM(1,M),M=1,45'
753 C          PRINT *, (RM(1,M),M=1,45)
754            WRITE(1,*)(RM(1,M),M=1,45)
755 C          PRINT *, (RM(1,M+45),M=1,45)
756             WRITE(1,*) 'SECOND SECTION RM(1,M+45),M=1,45'
757             WRITE(1,*)(RM(1,M+45),M=1,45)
758 C          PRINT *, (RM(46,M),M=1,45)
759            WRITE(1,*)'THIRD SECTION RM(46,M),M=1,45'
760             WRITE(1,*)(RM(46,M),M=1,45)
761 C          PRINT *, (RM(46,M+45),M=1,45)
762            WRITE(1,*)'FOURTH SECTION RM(46,M+45),M=1,45'
763              WRITE(1,*)(RM(46,M+45),M=1,45)
764 C
765 C
766            IFAIL=0
767           CALL F04ADF(RM,MLIM,RV,MLIM,MLIM,1,AV,MLIM,
768      *    WKSPCE,IFAIL)
769           IF(IFAIL.EQ.0) THEN
770             PRINT*,'SUCCESSFUL SOLUTION FOR (A) COEFFICIENTS.'
771           ELSE
772             PRINT*,'FAILURE TO SOLVE FOR (A) COEFFICIENTS.'
773           END IF
774 C         PRINT *, (AV(L),L,'AV',L=1,MLIM)
775           RETURN
776           END
777 C
778 C         ***********************************************************
779 C
780           SUBROUTINE FCOEFF(AV,FC,T)
781           PARAMETER (NLIM=-22, LIM=22, KLIM=45, MLIM=90  )
782           COMPLEX AV(MLIM),FC(KLIM),T(MLIM,MLIM)
783           REAL VR,VI
784           REWIND 13
785 C
786 C         CALCULATE THE FOURIER COEFFICIENTS OF THE PSEUDO-OBJECT
787 C         AND WRITE THE RESULTS ON UNIT15.
788 C         STORE THE FIRST LAYER EIGENVECTORS IN MATRIX T.
789 C
790           DO 920 L=1,KLIM
791             WRITE(15,*) AV(L),AV(L+KLIM),L
792             DO 910 M=1,KLIM
793               READ(13,*) VR,VI
794               T(L,M) = CMPLX(VR,VI)
795  910        CONTINUE
796  920      CONTINUE
797 C
798 C         CLEAR THE FC VECTOR AND SET THE FC(0) VALUE TO -1.0.
799 C         CALCULATE FOURIER SERIES COEFFICIENTS FC USING THE A-
800 C         COEFFICIENTS AND THE EIGENVECTORS. SEE EQ. 22 OF APPENDIX III.
```

```
801 C
802           DO 940 L=1,KLIM
803             IF(L.EQ.LIM+1) THEN
804               FC(L) = CMPLX(-1.0,0.0)
805             ELSE
806               FC(L) = CMPLX(0.0,0.0)
807             END IF
808             DO 930 M=1,KLIM
809               FC(L) = FC(L)+(AV(M)+AV(M+KLIM))*T(L,M)
810  930        CONTINUE
811  940      CONTINUE
812 C
813 C         THE FOURIER SERIES FOR THE PSEUDO-OBJECT IS WRITTEN ON
814 C         UNIT16, IN A FORMAT WHICH ALLOWS IT TO INTERFACE TO A
815 C         PLANAR IMAGING OR OTHER PROGRAM.
816 C
817           DO 950 K=1,KLIM
818             WRITE(16,999) FC(K)
819             PRINT*,FC(K)
820  950      CONTINUE
821  999      FORMAT(1X,2F20.8)
822           RETURN
823           END
824 C
825 C         **************************************************************
826 C
827           SUBROUTINE IMAGE(FC,PI,SPAFRE,TRA,DF,LSKIP,WAVE)
828           PARAMETER(NLIM=-22, LIM=22, KLIM=45, MLIM=90)
829           REAL PI,WAVE,SPAFRE,RR,RI,XPOS,TRA(2),
830      2       RIM(-600:600),IR,CAM(-100:100),ELEC(-500:500),X,YN,XI
831           COMPLEX FC(NLIM:LIM),CI,CCI,RT,FFC,FOC(-KLIM:KLIM)
832 C
833 C         THIS SUBROUTINE COMPUTES THE IMAGE OF THE LINE ASSUMING
834 C         ONE DIMENSIONAL OPTICS.
835 C
836 C         THE IMAGE IS COMPUTED FOR 1000 POINTS OVER A RANGE
837 C         OF +/- 0.5*THE PERIOD.
838 C
839           CI = CMPLX(0.0,1.0)
840 C
841 C         IF LSKIP = 1 THEN READ IN THE PREVIOUS COEFFICIENTS.
842 C
843           IF(LSKIP.EQ.1) THEN
844             DO 105 I=NLIM,LIM
845               READ(16,*) RR, RI
846               FC(I) = CMPLX(RR,RI)
847  105        CONTINUE
848           END IF
849 C
850 C         OBJ = NUMERICAL APERTURE OF THE OBJECTIVE.
```

```
851 C         CON = NUMERICAL APERTURE OF THE "CONDENSER"
852 C         (ILLUMINATION APERTURE).
853 C         THESE PARAMETERS ARE PRESENTLY SET FOR THE NBS LASER SYSTEM
854 C
855           OBJ = 0.85
856           CON = 0.17
857           FM = OBJ*LIM
858           FR = CON*LIM
859 C
860 C         THE DEFOCUS TERM DF ADDS A PHASE MODULATION TO THE
861 C         FOURIER SERIES.
862 C
863           CCI = CI*2.0*PI*SPAFRE
864           DO 115 I=-KLIM,KLIM
865             FOC(I) = CEXP(2.0*PI*CI*DF*(WAVE*I*SPAFRE)**2)
866  115      CONTINUE
867 C
868 C         THE IMAGE IS COMPUTED FOR AN ADDITIONAL 100 POINTS ON
869 C         EITHER SIDE IN ORDER TO ALLOW FOR CONVOLUTION WITH A
870 C         DETECTOR APERTURE OR IMPULSE RESPONSE.
871 C
872           DO 130 IX=-600,600
873             XPOS = IX/(SPAFRE*1000.0)
874             RIM(IX) = 0.0
875             DO 120 J=-FR,FR
876               RT = CMPLX(0.0,0.0)
877               DO 110 K=J-FM,J+FM
878                 IF(ABS(K).GT.LIM) THEN
879                   FFC = CMPLX(0.0,0.0)
880                 ELSE
881                   FFC = FC(K)*FOC(K-J)
882                 END IF
883                 RT = RT+FFC*CEXP(CCI*XPOS*K)
884  110          CONTINUE
885               RIM(IX) = RIM(IX)+REAL(RT)**2+AIMAG(RT)**2
886  120        CONTINUE
887  130      CONTINUE
888 C
889 C         THE ARRAY RIM() CONTAINS THE OPTICAL IMAGE PROFILE.
890 C
891 C         CONVOLVE THE IMAGE WITH THE DETECTOR LINE SPREAD
892 C         FUNCTION.
893 C         IF TRA(1) IS GREATER THAN 0.01 THEN A SLIT APERTURE IS
894 C         ASSUMED.
895 C         OTHERWISE IF TRA(2) IS GREATER THAN 0.05 THEN A VIDEO
896 C         CAMERA WITH A GAUSSIAN LINE SPREAD FUNCTION IS ASSUMED.
897 C         IF BOTH ARE ZERO THEN NO CONVOLUTION TAKES PLACE.
898 C         THE ARRAY CAM() CONTAINS THE VIDEO CAMERA RESPONSE.
899 C         THE ARRAY ELEC() CONTAINS THE ELECTRICAL OUTPUT SIGNAL
900 C         OF THE TRANSDUER.
```

```
901 C
902            IF(TRA(1).GT.0.01) THEN
903              IR = TRA(1)*SPAFRE*500.0
904              IF(IR.GT.100) THEN
905                IR = 100
906              ELSE IF(IR.LT.1) THEN
907                IR = 1
908              END IF
909              DO 150 I=-500,500
910                ELEC(I) = 0.0
911                DO 140 J=-IR,IR
912                  ELEC(I) = ELEC(I)+RIM(J+I)
913  140           CONTINUE
914  150         CONTINUE
915            ELSE IF(TRA(2).GT.0.05) THEN
916              DO 160 I=-100,100
917                X = I/(SPAFRE*1000)
918                CAM(I) = EXP(-0.5*(X**2)/(TRA(2)**2))
919  160         CONTINUE
920              DO 180 I=-500,500
921                ELEC(I) = 0.0
922                DO 170 J=-100,100
923                  ELEC(I) = ELEC(I)+CAM(J)*RIM(I+J)
924  170           CONTINUE
925  180         CONTINUE
926            ELSE
927              DO 190 I=-500,500
928                ELEC(I) = RIM(I)
929  190         CONTINUE
930            END IF
931 C
932 C          WRITE THE OUTPUT IMAGE DATA ON UNIT17.
933 C
934 C          THE IMAGE IS NORMALISED WITH RESPECT TO THE INTENSITY AT
935 C          A DISTANCE OF 1/2 THE PERIOD AWAY FROM THE ORIGIN.
936 C
937            YN = AMAX1(ELEC(0),ELEC(500))
938            DO 195 I=-500,500
939              XI = I/(SPAFRE*1000.0)
940              ELEC(I) = ELEC(I)/YN
941              WRITE(17,*) ELEC(I),XI
942  195       CONTINUE
943 C
944 C          THE FOLLOWING 'END OF DATA' STATEMENT IS FOR THE
945 C          'DATAPLOT' GRAPHICS PACKAGE.
946 C
947            WRITE(17,*) 'END OF DATA'
948            RETURN
949            END
```

Appendix II
Test Cases for Thick Layer Imaging Program (THKIMAG)

Test Case #1: THICK DIELECTRIC LAYER WITH VERTICAL EDGES (6 µm wide line with vertical edges patterned in a 0.65 µm thick silicon dioxide layer on a silicon substrate).

```
1 0.53          12.0         1              : WAVELENGTH, PERIOD, NUMBER OF LAYERS
2 (1.00,0.00)   (4.10,0.06)  0              : RI(AIR), RI(SUBSTRATE), ID
3 6.00          0.00         0.00   0.00    : WIDTH, 3 POLYNOMINAL COEFFICIENTS
4 0.00          0.00         0.00           : DISPLACEMENTS IN Z
5 (1.46,0.0)    0.65                        : RI(PATTERNED LAYER), LAYER THICKNESS
6 0.20          0.00                        : SLIT WIDTH, CAMERA WIDTH
7 0             0.00                        : SKIP, DEFOCUS
```

Test Case #1: File FCOFPO: Fourier Coefficients of the Pseudo-Object

1	-.09108273	.00519622
2	-.06079249	.01308535
3	.00478018	.01658667
4	.04455374	.00100212
5	.00810522	-.00558479
6	-.03495132	-.01667204
7	-.00672853	.00298502
8	.01767570	.02462243
9	.00840075	-.00504291
10	-.00193394	-.02052349
11	-.01237166	.00493059
12	-.00605733	.00957640
13	.01508445	-.00253726
14	.00599687	.00264588
15	-.01573390	-.00030316
16	-.00008822	-.01386078
17	.01502888	.00264068
18	-.01048221	.02557344
19	-.01386187	-.00424937
20	.02992448	-.04556850
21	.01290886	.00491631
22	-.10926479	.13891567
23	.39447293	.04366360
24	-.10926479	.13891567
25	.01290886	.00491631
26	.02992448	-.04556850
27	-.01386187	-.00424937
28	-.01048221	.02557344
29	.01502888	.00264068
30	-.00008822	-.01386078
31	-.01573390	-.00030316
32	.00599687	.00264588
33	.01508445	-.00253726
34	-.00605733	.00957640
35	-.01237166	.00493059
36	-.00193394	-.02052349
37	.00840075	-.00504291
38	.01767570	.02462243
39	-.00672853	.00298502
40	-.03495132	-.01667204
41	.00810522	-.00558479
42	.04455374	.00100212
43	.00478018	.01658667
44	-.06079249	.01308535
45	-.09108273	.00519622

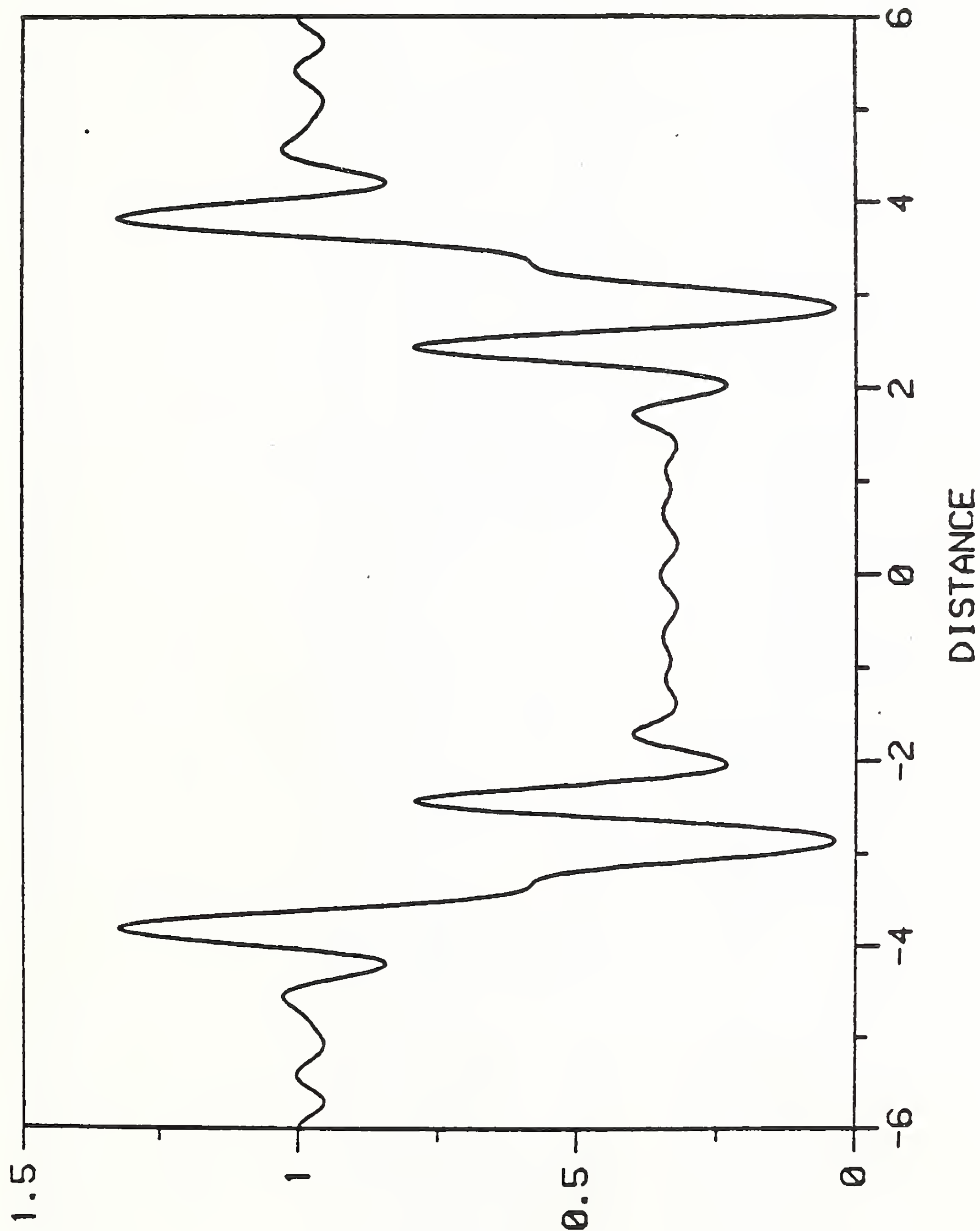
CASE1 PROFILE FOR DN THKIMAG
1.5
1
0.5
0
-6
-4
-2
0
2
4
6
DISTANCE

Test Case #2: THIN METAL LAYER WITH VERTICAL EDGES
(6 µm wide line with vertical edges patterned in a 0.09 µm thick chromium layer on a silicon substrate).

```
1  0.53          12.0          1          : WAVELENGTH, PERIOD, NUMBER OF LAYERS
2 (1.00,0.00)   (4.10,0.06)    0          : RI(AIR), RI(SUBSTRATE), ID
3 6.00           0.00          0.00  0.00 : WIDTH, 3 POLYNOMINAL COEFFICIENTS
4 0.00           0.00          0.00       : DISPLACEMENTS IN Z
5 (1.40,2.55)    0.09                     : RI(PATTERNED LAYER), LAYER THICKNESS
6 0.20           0.00                     : SLIT WIDTH, CAMERA WIDTH
7 0              0.00                     : SKIP, DEFOCUS
```

Test Case #2: File FCOFPO: Fourier Coefficients of the Pseudo-Object

1	.02598611	-.01092292
2	-.01353529	.00904450
3	-.01731358	.00311739
4	.01756685	-.00795909
5	.01356888	-.00057359
6	-.02047819	.00686085
7	-.01107900	-.00064297
8	.02327938	-.00598552
9	.00921602	.00126586
10	-.02648625	.00536360
11	-.00773381	-.00157148
12	.03061512	-.00501271
13	.00650267	.00169434
14	-.03646409	.00498365
15	-.00544231	-.00171108
16	.04564310	-.00541449
17	.00449766	.00167165
18	-.06227954	.00669869
19	-.00362787	-.00161367
20	.10149616	-.01032568
21	.00279663	.00156888
22	-.29965151	.02984478
23	-.14235833	-.46645156
24	-.29965151	.02984478
25	.00279663	.00156888
26	.10149616	-.01032568
27	-.00362787	-.00161367
28	-.06227954	.00669869
29	.00449766	.00167165
30	.04564310	-.00541449
31	-.00544231	-.00171108
32	-.03646409	.00498365
33	.00650267	.00169434
34	.03061512	-.00501271
35	-.00773381	-.00157148
36	-.02648625	.00536360
37	.00921602	.00126586
38	.02327938	-.00598552
39	-.01107900	-.00064297
40	-.02047819	.00686085
41	.01356888	-.00057359
42	.01756685	-.00795909
43	-.01731358	.00311739
44	-.01353529	.00904450
45	.02598611	-.01092292

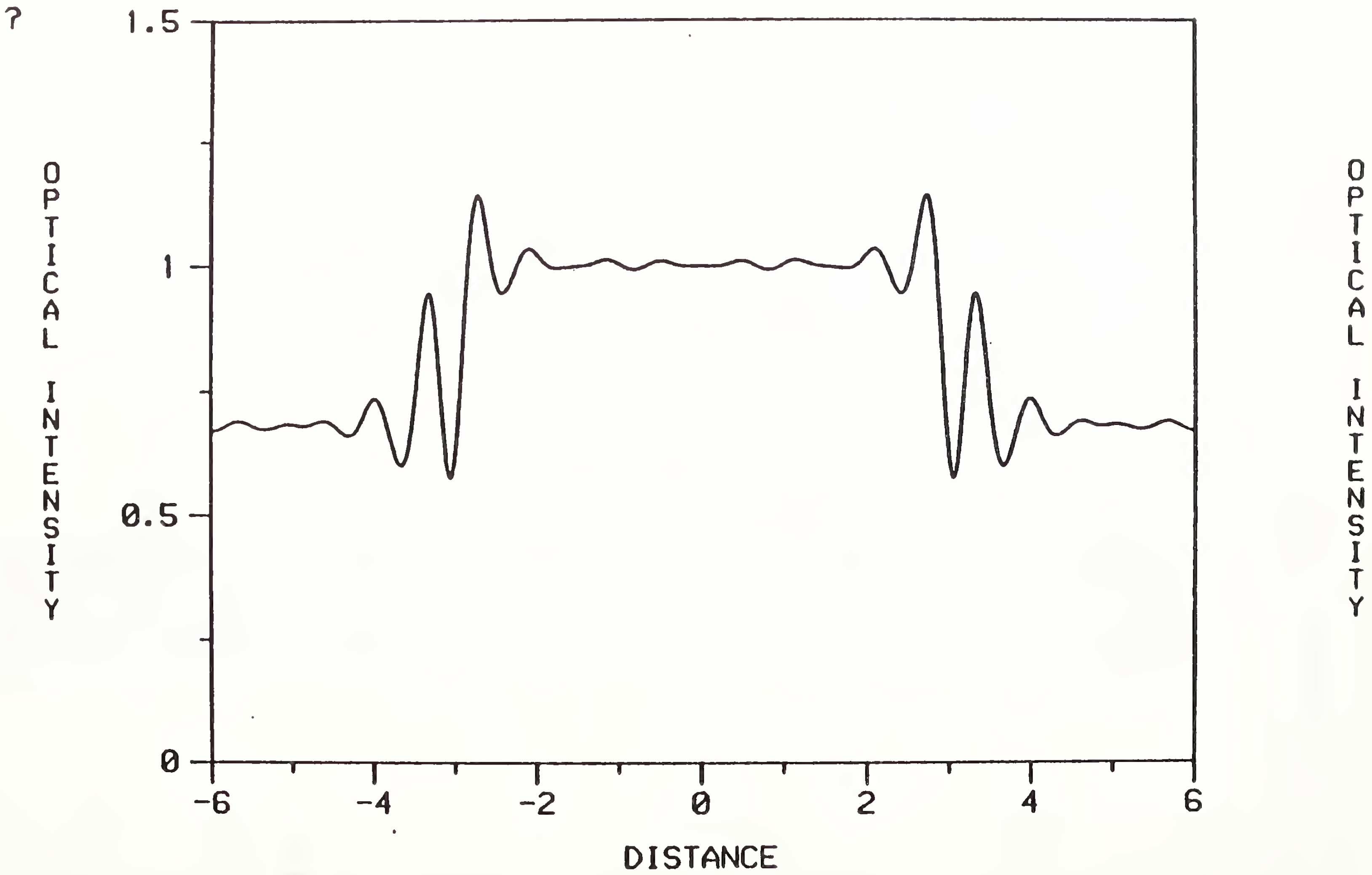
CASE2,ONE LAYER, 3/20/87, THKBEST
OPTICAL INTENSITY
1.5
1
0.5
0
-6
-4
-2
0
2
4
6
DISTANCE
OPTICAL INTENSITY

Test Case #3: THICK DIELECTRIC LAYER WITH CURVED EDGES.
(6 μm wide line with curved edges patterned in a 0.65 μm thick silicon dioxide layer on a silicon substrate).

```
1 0.53        12.0        9           : WAVELENGTH, PERIOD, NUMBER OF LAYERS
2 (1.00,0.00) (4.10,0.06) 0           : RI(AIR), RI(SUBSTRATE), ID
3 6.00        0.00        2.00   0.00 : WIDTH, 3 POLYNOMINAL COEFFICIENTS
4 0.00        0.00        0.00        : DISPLACEMENTS IN Z
5 (1.46,0.00) 0.65                    : RI(PATTERNED LAYER), LAYER THICKNESS
6 0.20        0.00                    : SLIT WIDTH, CAMERA WIDTH
7 0           0.00                    : SKIP, DEFOCUS
```

Test Case #3: File PARFIL: Parameter File Created

```
 1   RUN PARAMETERS.
 2   WAVELENGTH = .53
 3   NUMBER OF LAYERS=9.
 4   WAVE NUMBER =11.85506661732
 5   AIR LAYER =(1.,0.)
 6   SUBSTRATE =(4.1,.06)
 7   DEFOCUS =0.
 8   SLIT WIDTH IN MICRONS =.2
 9   CAMERA WIDTH PARAMETER =0.
10   LAYER      WIDTH      POSITION        RI          OFFSET
11    1         6.003        .072      1.460   .000          .000
12    2         6.023        .144      1.460   .000          .000
13    3         6.065        .217      1.460   .000          .000
14    4         6.128        .289      1.460   .000          .000
15    5         6.211        .361      1.460   .000          .000
16    6         6.316        .433      1.460   .000          .000
17    7         6.441        .506      1.460   .000          .000
18    8         6.587        .578      1.460   .000          .000
19    9         6.754        .650      1.460   .000          .000
```

Test Case #3: File FCOFPO: Fourier Coefficients of the Pseudo-Object

1	.03128047	-.04799119
2	-.00117774	-.02619416
3	-.04538472	.02843279
4	.00285586	-.00315021
5	.04860053	.01296409
6	-.01663746	-.01247821
7	-.02455180	-.02653567
8	.00370391	.02884274
9	.01005389	.01942759
10	.01510389	-.02721254
11	-.00775574	-.00992680
12	-.02538226	.01395119
13	.01109421	.00413423
14	.02493682	.00192007
15	-.01569382	-.00211696
16	-.01660809	-.01617415
17	.01970374	.00272111
18	.00248225	.02957102
19	-.02276161	-.00472439
20	.02118083	-.04960428
21	.02524568	.00671538
22	-.10579441	.14143811
23	.38000129	.04024071
24	-.10579441	.14143811
25	.02524568	.00671538
26	.02118083	-.04960428
27	-.02276161	-.00472439
28	.00248225	.02957102
29	.01970374	.00272111
30	-.01660809	-.01617415
31	-.01569382	-.00211696
32	.02493682	.00192007
33	.01109421	.00413423
34	-.02538226	.01395119
35	-.00775574	-.00992680
36	.01510389	-.02721254
37	.01005389	.01942759
38	.00370391	.02884274
39	-.02455180	-.02653567
40	-.01663746	-.01247821
41	.04860053	.01296409
42	.00285586	-.00315021
43	-.04538472	.02843279
44	-.00117774	-.02619416
45	.03128047	-.04799119

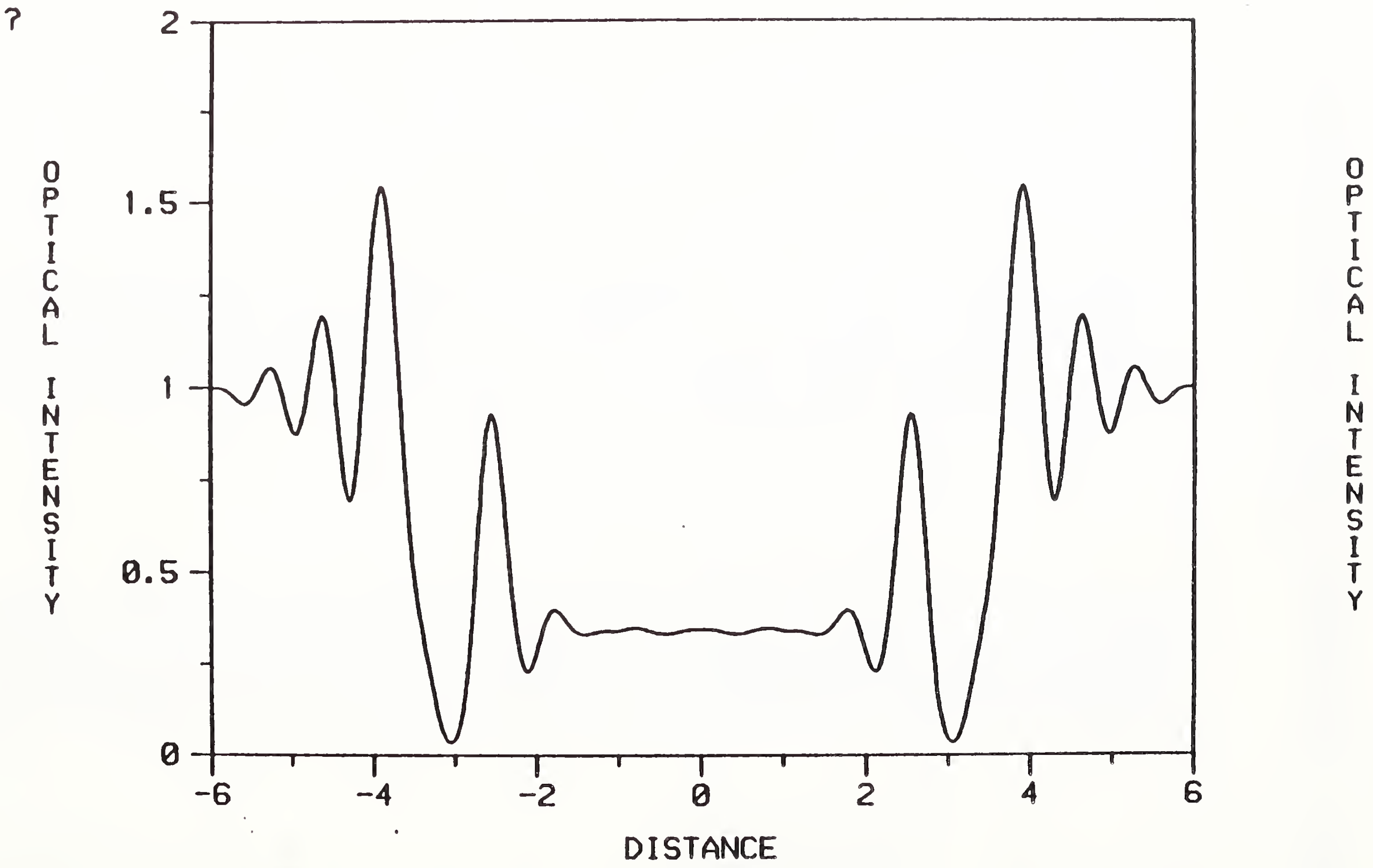

CASE3N, 2/22/87, THKBEST
OPTICAL INTENSITY
OPTICAL INTENSITY
2
1.5
1
0.5
0
-6
-4
-2
0
2
4
6
DISTANCE

Test Case #4: THICK METAL LAYER WITH VERTICAL EDGES

(6 µm wide line with vertical edges patterned in a 0.6 µm thick chromium layer on a silicon substrate).

```
1 0.53          12.0          1              : WAVELENGTH, PERIOD, NUMBER OF LAYERS
2 (1.00,0.00) (4.10,0.06)  0              : RI(AIR), RI(SUBSTRATE), ID
3 6.00          0.00          0.00   0.00 : WIDTH, 3 POLYNOMINAL COEFFICIENTS
4 0.00          0.00          0.00           : DISPLACEMENTS IN Z
5 (1.40,2.55) 0.60                         : RI(PATTERNED LAYER), LAYER THICKNESS
6 0.20          0.00                         : SLIT WIDTH, CAMERA WIDTH
7 0             0.00                         : SKIP, DEFOCUS
```

Test Case #4: File FCOFPO: Fourier Coefficients of the Pseudo-Object

1	.02870492	-.00727836
2	-.03936288	-.01604885
3	.00858718	.02754465
4	.02527876	.00266374
5	-.01939032	-.03161583
6	-.00720966	.00412280
7	.01258914	.04300149
8	-.00154677	-.02651014
9	.00149106	-.03863546
10	-.00367560	.04706727
11	-.00975738	.02263821
12	.01454326	-.05862991
13	.01080683	-.00255415
14	-.02546317	.06130368
15	-.00753362	-.01701846
16	.03522425	-.05701120
17	.00344633	.03333270
18	-.04739825	.04842201
19	-.00070328	-.04416899
20	.07514600	-.04152960
21	-.00182714	.04869017
22	-.21542281	.06822844
23	-.26974701	-.56211569
24	-.21542281	.06822866
25	-.00182724	.04869002
26	.07514611	-.04152962
27	-.00070319	-.04416899
28	-.04739853	.04842213
29	.00344651	.03333271
30	.03522438	-.05701149
31	-.00753393	-.01701814
32	-.02546294	.06130364
33	.01080669	-.00255426
34	.01454345	-.05863000
35	-.00975762	.02263852
36	-.00367547	.04706706
37	.00149104	-.03863546
38	-.00154668	-.02651021
39	.01258891	.04300184
40	-.00720944	.00412244
41	-.01939040	-.03161581
42	.02527873	.00266401
43	.00858720	.02754443
44	-.03936286	-.01604884
45	.02870492	-.00727828

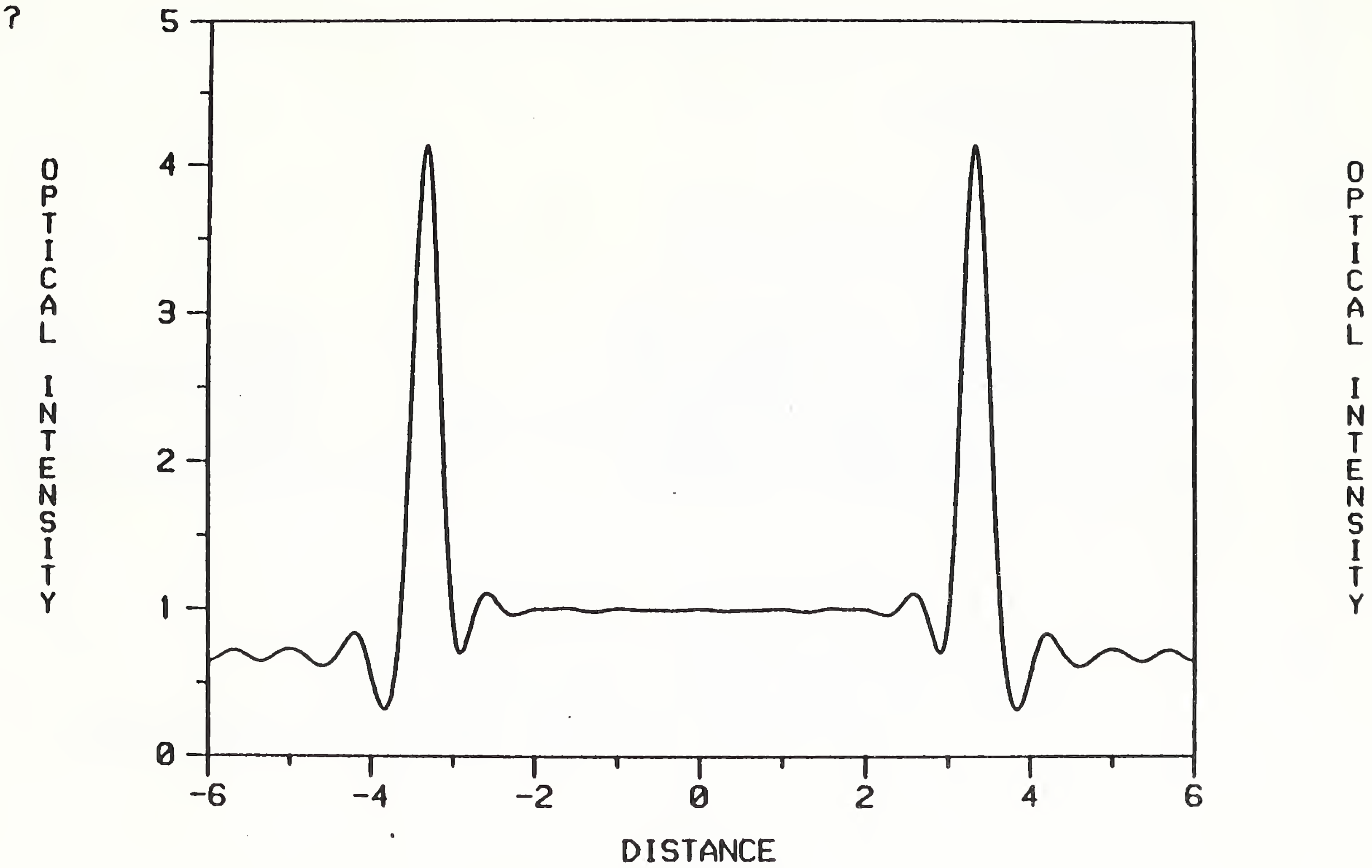
CASE4, 2/22/87, THKBEST
?
OPTICAL INTENSITY
0
1
2
3
4
5
-6
-4
-2
0
2
4
6
DISTANCE
OPTICAL INTENSITY

Test Case #5: THICK METAL LAYER WITH CURVED EDGES
(6 μm wide line with curved edges patterned in a 0.60 μm thick silicon dioxide layer on a silicon substrate).

```
1 0.53          12.0          9              : WAVELENGTH, PERIOD, NUMBER OF LAYERS
2 (1.00,0.00) (4.10,0.06)   0              : RI(AIR), RI(SUBSTRATE), ID
3 6.00          0.00          2.00   0.00  : WIDTH, 3 POLYNOMINAL COEFFICIENTS
4 0.00          0.00          0.00         : DISPLACEMENTS IN Z
5 (1.40,2.55) 0.60                         : RI(PATTERNED LAYER), LAYER THICKNESS
6 0.20          0.00                       : SLIT WIDTH, CAMERA WIDTH
7 0             0.00                       : SKIP, DEFOCUS
```

- Test Case #5: File PARFIL: Parameter File Created

```
 1  RUN PARAMETERS.
 2  WAVELENGTH = .53
 3  NUMBER OF LAYERS=9.
 4  WAVE NUMBER =11.85506661732
 5  AIR LAYER =(1.,0.)
 6  SUBSTRATE =(4.1,.06)
 7  DEFOCUS =0.
 8  SLIT WIDTH IN MICRONS =.2
 9  CAMERA WIDTH PARAMETER =0.
10  LAYER      WIDTH     POSITION       RI        OFFSET
11   1         6.002       .067     1.400 2.550         .000
12   2         6.020       .133     1.400 2.550         .000
13   3         6.056       .200     1.400 2.550         .000
14   4         6.109       .267     1.400 2.550         .000
15   5         6.180       .333     1.400 2.550         .000
16   6         6.269       .400     1.400 2.550         .000
17   7         6.376       .467     1.400 2.550         .000
18   8         6.500       .533     1.400 2.550         .000
19   9         6.642       .600     1.400 2.550         .000
```

Test Case #5: File FCOFPO: Fourier Coefficients of the Pseudo-Object

1	.02859869	.01883469
2	-.01777494	-.05351227
3	-.01575921	.07268917
4	.01125702	-.04988998
5	.03861030	.00407903
6	-.05863673	.02278771
7	.00882784	-.01948456
8	.04261764	.00856627
9	-.02643598	-.00272235
10	-.01766390	-.00659771
11	.01759161	.01642617
12	.00861215	-.00775205
13	-.00318939	-.01494420
14	-.01427936	.01811821
15	-.00661590	.00686578
16	.02942126	-.02111680
17	.00859497	-.00085589
18	-.05174989	.02242236
19	-.00051795	-.00098279
20	.08337158	-.03235164
21	-.01442410	.00796601
22	-.20644118	.07115434
23	-.27539556	-.53212378
24	-.20644114	.07115399
25	-.01442399	.00796627
26	.08337133	-.03235159
27	-.00051788	-.00098292
28	-.05174964	.02242235
29	.00859462	-.00085587
30	.02942143	-.02111668
31	-.00661589	.00686571
32	-.01427944	.01811798
33	-.00318921	-.01494381
34	.00861184	-.00775220
35	.01759189	.01642605
36	-.01766396	-.00659770
37	-.02643602	-.00272207
38	.04261751	.00856600
39	.00882814	-.01948459
40	-.05863689	.02278783
41	.03861020	.00407919
42	.01125717	-.04989043
43	-.01575919	.07268954
44	-.01777511	-.05351234
45	.02859880	.01883462

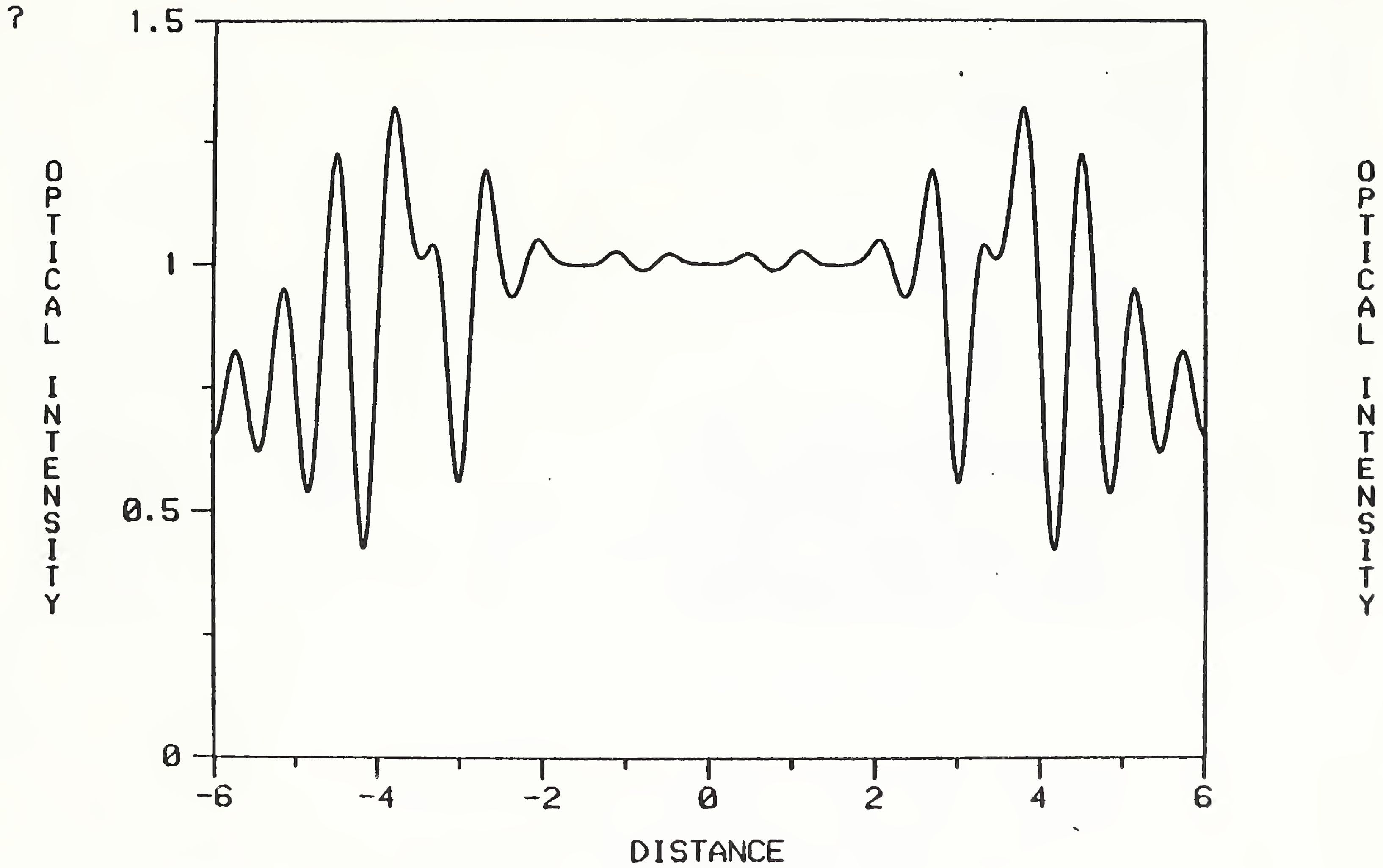
CASE5, 2/22/87, THKBEST
OPTICAL INTENSITY
OPTICAL INTENSITY
1.5
1
0.5
0
-6
-4
-2
0
2
4
6
DISTANCE

Test Case #6: THICK POLYSILICON LAYER WITH CURVED EDGES
(6 μm wide line with curved edges patterned in a 0.6 μm thick polysilicon layer on a silicon substrate).

```
1 0.53          12.0          9              : WAVELENGTH, PERIOD, NUMBER OF LAYERS
2 (1.00,0.00) (4.10,0.06)   0              : RI(AIR), RI(SUBSTRATE), ID
3 6.00          0.00          2.00   0.00 : WIDTH, 3 POLYNOMINAL COEFFICIENTS
4 0.00          0.00          0.00           : DISPLACEMENTS IN Z
5 (3.80,0.10) 0.60                         : RI(PATTERNED LAYER), LAYER THICKNESS
6 0.20          0.00                         : SLIT WIDTH, CAMERA WIDTH
7 0             0.00                         : SKIP, DEFOCUS
```

Test Case #6: File PARFIL: Parameter File Created

```
 1  RUN PARAMETERS.
 2  WAVELENGTH = .53
 3  NUMBER OF LAYERS=9.
 4  WAVE NUMBER =11.85506661732
 5  AIR LAYER =(1.,0.)
 6  SUBSTRATE =(4.1,.06)
 7  DEFOCUS =0.
 8  SLIT WIDTH IN MICRONS =.2
 9  CAMERA WIDTH PARAMETER =0.
10  LAYER      WIDTH      POSITION       RI         OFFSET
11   1         6.002        .067     3.800   .100         .000
12   2         6.020        .133     3.800   .100         .000
13   3         6.056        .200     3.800   .100         .000
14   4         6.109        .267     3.800   .100         .000
15   5         6.180        .333     3.800   .100         .000
16   6         6.269        .400     3.800   .100         .000
17   7         6.376        .467     3.800   .100         .000
18   8         6.500        .533     3.800   .100         .000
19   9         6.642        .600     3.800   .100         .000
```

Test Case #6: File FCOFPO: Fourier Coefficients of the Pseudo-Object

1	-.06445069	.00175338
2	.10217661	-.01417309
3	-.06446184	.01696297
4	-.03134388	-.00120886
5	.07807896	-.01799169
6	-.01812634	.01902242
7	-.06195582	-.00139914
8	.04708281	-.01378403
9	.03549830	.01048018
10	-.05741779	.00419147
11	-.01086065	-.01166372
12	.05640716	.00465509
13	-.00874018	.00740007
14	-.04823824	-.01104616
15	.02114851	.00151754
16	.03683013	.01295479
17	-.02419279	-.01478962
18	-.02814956	-.00686661
19	.01508793	.03343811
20	.03801847	-.01927935
21	.00830037	-.06197198
22	-.16673161	.17059941
23	-.31875250	-.22803972
24	-.16673161	.17059941
25	.00830037	-.06197198
26	.03801847	-.01927935
27	.01508793	.03343811
28	-.02814956	-.00686661
29	-.02419279	-.01478962
30	.03683013	.01295479
31	.02114851	.00151754
32	-.04823824	-.01104616
33	-.00874018	.00740007
34	.05640716	.00465509
35	-.01086065	-.01166372
36	-.05741779	.00419147
37	.03549830	.01048018
38	.04708281	-.01378403
39	-.06195582	-.00139914
40	-.01812634	.01902242
41	.07807896	-.01799169
42	-.03134388	-.00120886
43	-.06446184	.01696297
44	.10217661	-.01417309
45	-.06445069	.00175338

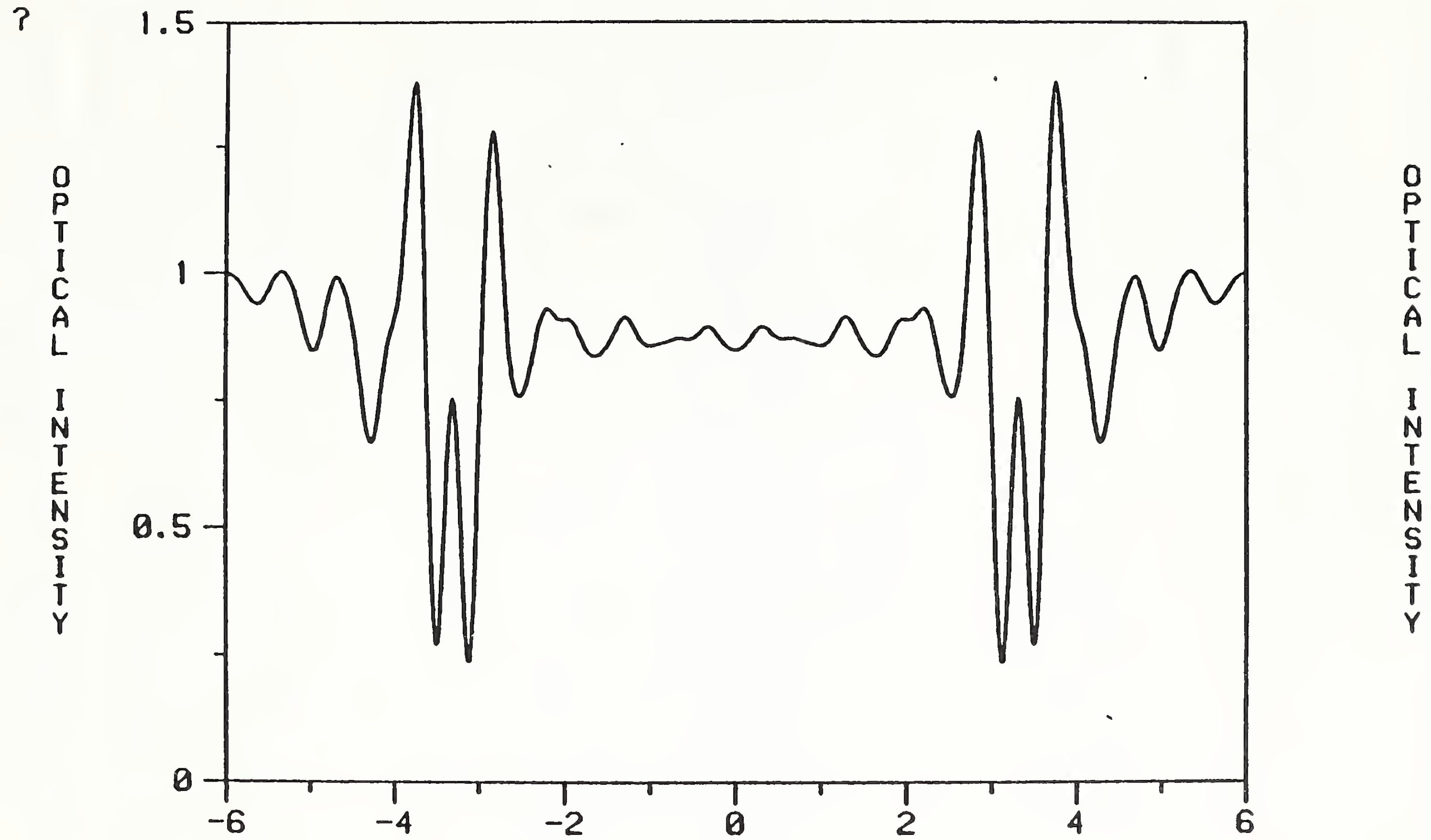

OPTICAL INTENSITY

Appendix III

Reprint - "Modeling of the optical microscope image of lines patterned in thick layers with variable edge geometry," by D. Nyyssonen and C. P. Kirk (submitted to J. Opt. Soc. Am.).

Modeling of the optical microscope imaging of lines patterned in thick layers with variable edge geometry*

Diana Nyyssonen**
National Bureau of Standards, Gaithersburg, MD 20899

Chris P. Kirk†
Vickers Instruments, Haxby Road, York. Y03 7SD. England
and
Department of Electrical and Electronic Engineering,
Leeds University, Leeds. LS2 9JT. England

Abstract

A monochromatic, waveguide model is presented which can predict the optical microscope images of line objects with arbitrary edge geometry, patterned in thick-layers including multilayer structures with sloping, curved, and undercut edges, granular structures such as lines patterned in polysilicon, as well as asymmetric objects. The model is used to illustrate the effects of line edge structure on the optical image. Qualitative agreement with experimentally obtained optical image profiles is demonstrated. Application of the model to study the effects of variations in layer thickness and edge geometry on linewidth measurements made at different stages of manufacturing integrated-circuit devices is discussed.

---

* Contribution of the National Bureau of Standards; not subject to copyright.
This work was performed under the Research Associate Agreement (CN-454) between the National Bureau of Standards and Vickers Instruments, July 1984.
** Currently with CD Metrology, Inc., Germantown, MD 20874.
† Currently with KLA Instruments, San Jose, CA 95131.

INTRODUCTION

During the manufacture of integrated circuit wafers, critical dimensions of certain features must be measured at different stages of the production process. The control of the critical dimension of linewidth is usually monitored by using an optical or scanning-electron microscope. The measurements made by a correctly aligned microscope fitted with an appropriate measurement attachment are usually limited in accuracy and precision not by instrumental errors but by the lack of understanding of the characteristics of the image profile and the lack of accurate edge detection algorithms.

In the past, optical imaging in the microscope has been described by the scalar theory of partially coherent imaging [1-3] which characterizes the object by a planar complex transmittance or reflectance function. However, this approach does not accurately predict either the scattered field or the image structure for micrometer-sized line objects thicker than approximately one-quarter of the illuminating wavelength [3]. Unfortunately, most of the line features to be measured during the production of integrated circuits fall into this category of thick objects. Typical line objects are patterned in layers with thicknesses ranging from 0.3 to over 1.0 µm (e.g. photoresist).

Integrated-circuit features encompass a wide variety of materials including dielectrics and absorbing materials of high and low conductivity (e.g., semiconductors in crystalline and amorphous states with varying amounts of dopant impurities, refractory metals, etc.) and line geometries with edge shapes varying from vertical to the complex shapes shown in Fig. 1. These lines may be etched into layers and be situated on top of metal or dielectric layers. Because of this wide variation, most of the approaches found in the literature are of only limited usefulness.

Scattering from micrometer-sized thick objects with complex indices of refraction falls in the domain of scattering by objects whose size is comparable to the illuminating wavelength such as Mie scattering [4] and requires an electromagnetic field treatment to accurately predict the scattered field. The various approaches that have been used to treat scattering by objects on the order of a wavelength can be found in the large volume of papers primarily in the areas of scattering by particles [5], scattering by surfaces with defects or protuberances [6], or diffraction by gratings [7]. Many of these approaches are limited either to objects of specific shapes [4,8] or weakly scattering objects which satisfy either the Rayleigh [9] or Born [10] approximations, or require infinite conductivity or specific grating geometries. Many are mathematically cumbersome when applied to the wide range of object shapes and materials of present interest.

Recently, the problem of imaging of line objects with vertical edge walls patterned in thick layers of dielectrics and metals was treated by Nyyssonen [3,11] who developed a model based on the waveguide analysis for thick dielectric structures of Burckhardt [12]. Burckhardt's model was originally developed for diffraction from sinusoidal dielectric gratings and was applied to the reconstruction of bleached holograms. Kaspar [13,14] extended Burckhardt's approach to include absorbing photographic emulsions and non-sinusoidal grating structures and applied this approach to contact printing as well. Kaspar's work related the dielectric constant of the grating to the photographic density of the film.

The waveguide model previously used by Nyyssonen [3,11] assumes that the line structure is patterned in a nonmagnetic layer which can be characterized by its complex index of refraction which is taken to be constant with depth within the layer. Thus, this model can be used to represent homogeneous line structures with

vertical edge walls. The spatial function representing the variation in the dielectric constant (square of the complex index of refraction) in the layer is expanded in a Fourier series. When this is substituted into the wave equation, Hill's equation [15] is obtained. The eigenvalue solutions to this equation represent waveguide modes. Assuming a single incident plane wave normal to the surface, the boundary value problem at the layer interfaces is solved to determine the Fourier coefficients in the expansions for the transmitted and reflected fields. This method allows the use of conventional scalar imaging theory to compute the image when no polarization effects are present. In such a case, the E- and H-field components are equivalent and either may be used in the scalar imaging equations.

In this paper, the waveguide model is extended to line objects whose index of refraction and geometry vary with depth in the layer, thus enabling line objects with nonvertical edges and multilayer structures to be considered. This extension of the model allows the images of virtually all line structures commonly encountered in IC fabrication to be modeled.

Thick-layer Model for Variable Edge Geometry

The method of solution for line structures of arbitrary edge geometry whose index of refraction may vary with depth in the layer is an extension of Nyyssonen's earlier method used for vertical edge walls discussed above. A line object of the type to be treated in this paper is shown in Fig. 2a. This line structure has been chosen because it contains different materials, curved edges, asymmetry, and an unpatterned sub-layer. The line structure in the patterned layer varies in both width and dielectric constant as a function of depth z within the layer. Figure 2b shows how this line structure may be approximated by a multilayer set of line objects each of which has a constant index of refraction over a small interval of depth z. The line may thus

be represented by a set of layers with the complex dielectric constant ε in each layer represented by the Fourier series expansion of:

$$\varepsilon_n(x) = \begin{cases} \hat{n}_n^{\,2}, & \left(\frac{-W_n}{2} + \Delta_n\right) < x < \left(\frac{W_n}{2} + \Delta_n\right) \\ 1, & \text{between the lines} \end{cases} \tag{1}$$

where:

$\hat{n}_n$ = refractive index of the nth layer of the line structure,
W_n = width of the nth layer, and
Δ_n = offset of the nth layer in the x-direction. (See Fig. 2b)

Nonperiodic structures are taken as periodic with a very large repeating distance (period).

The eigenvalue solutions for the electromagnetic field components are found independently for each layer. The boundary value equations at each interface form a set of complex matrix equations which when solved allow the substitution of a single "equivalent" scattering layer for the multilayer structure. Thereafter, the solution for the transmitted and reflected field components and image are found in the same manner as for the single layer case [3,11].

Following Burckhardt's method [12] and assuming monochromatic illumination where $\underline{E} = \underline{E}_o e^{-i\omega t}$, we start with the inhomogeneous wave equation for either the $\underline{E}$- or $\underline{H}$-field [16]:

$$^2\underline{E} + \hat{\varepsilon}\mu k_o^2\underline{E} + \text{grad}\ \frac{\underline{E}}{\hat{\varepsilon}} \cdot \text{grad}\ \hat{\varepsilon} = 0 \tag{2}$$

$$^2\underline{H} + \hat{\varepsilon}\mu k_o^2\underline{H} + \frac{\text{grad}\ \hat{\varepsilon}}{\hat{\varepsilon}} \times \text{curl}\ \underline{H} = 0 \tag{3}$$

with $k_o^2\hat{\varepsilon}\mu = k_o^2\hat{\eta}^2$ for nonmagnetic media.

If we choose the (x,y,z)-axes as we have done so that $\hat{\varepsilon}$ is constant along the length of the line in the y-direction, for TE-mode ($\underline{E} = E_y\underline{y}$) and TM-mode ($\underline{H} = H_y\underline{y}$) respectively, these equations simplify to

$$\nabla^2 E_y + k_o^2\hat{\varepsilon}E_y = 0 \qquad \text{(TE-mode)} \qquad (4)$$

and

$$\nabla^2 H_y - \frac{1}{\hat{\varepsilon}}\frac{\partial\varepsilon}{\partial x}\frac{H_y}{\partial x} + k_o^2\hat{\varepsilon}H_y = 0 \qquad \text{(TM-mode)} \qquad (5)$$

In the following analysis we consider only TE-mode because in the experimental NBS laser linewidth measuring system, the direction of polarization of the laser source is aligned parallel to the y-direction in the sample plane and the x-direction is the image scan direction. See Fig. 3. However, for any other system configuration and mode of illumination, the field can be considered as a superposition of TE- and TM-modes [17] and the corresponding analysis for TM-mode will be required. See ref. 12. Note that these modes are determined with respect to the orientation of the structure (not the incident wave) and are uncoupled (TE-mode: E_y, H_x, H_z, TM-mode H_y, E_x, E_z).

The solution for the TE-mode is taken in the form $E_y(x,z) = X(x)\,Z(z)$ and since $\hat{\varepsilon}=\hat{\varepsilon}(x)$, the method of separation of variables using a separation constant α results in

$$\frac{\partial^2 X(x)}{\partial x^2} + k_o^2\hat{\varepsilon}(x)X(x) + \alpha^2 X(x) = 0 \qquad (6)$$

$$\frac{\partial^2 Z}{\partial z^2} = \alpha^2 Z(z) \tag{7}$$

These equations hold for any functional form of $\hat{\varepsilon}(x)$. However, following Burckhardt, we choose the Fourier approach where $\hat{\varepsilon}_n(x)$ from eq. (1) is represented by the Fourier series

$$\hat{\varepsilon}_n(x) = \sum_q E_{q,n} \exp(2\pi iqx/P) \tag{8}$$

where

$$E_{q,n} = \begin{cases} (W_n/P)\hat{n}_n^2 + (1-W_n/P)\hat{n}_0^2 & q=0 \\ \dfrac{(\hat{n}_n^2-\hat{n}_0^2)}{q\pi} \exp(2\pi i\, \Delta_n q/P)\sin(q\pi W_n/P) & q\neq 0 \end{cases}$$

where P is the period chosen arbitrarily large when the object consists of a single line and q is the summation index. Substituting eq. (8) into eq. (6) yields the differential equation known as Hill's equation

$$\frac{\partial^2 X(x)}{\partial x^2} + k_0^2 \left[\sum_q E_{q,n}\exp(2\pi iqx/P)\right] X(x) + \alpha^2 X(x) = 0 \tag{9}$$

The solution for this general form of Hill's equation is given by Kaspar and others [13,15]. The form of the eigenvalue matrix is given in the Appendix. The solution of eq. (9) for the n-th layer is of the form

$$E_y^n(x,z) = \sum_m \left[A_{m,n}\exp(\alpha_{m,n}z) + A'_{m,n}\exp(-\alpha_{m,n}z)\right] \cdot \sum_j B_{j,m,n}\exp(2\pi ijx/P) \tag{10}$$

where the $\alpha_{m,n}$'s are the eigenvalues and the $B_{j,m,n}$'s are the eigenvector solutions to Hill's equation. The $A_{m,n}$ and $A'_{m,n}$ are weighting constants which must be determined from the boundary conditions. Each of these terms represents an inhomogeneous plane wave or waveguide mode which is supported by the line structure. Note that, when there is no absorption, ($\hat{\eta}$ real) the eigenvalues are purely imaginary and this form reduces to that of Burckhardt.

The solution for the transmitted and reflected fields is found by equating the tangential components of the $\underline{E}$- and $\underline{H}$-fields at each layer interface. The x-component of the $\underline{H}$-field is found from $ik_o \underline{H} = \text{curl } \underline{E}$ or, here, $ik_o H_x = -\partial E_y/\partial z$:

$$H_x^n(x,z) = \sum_m \left[A_{m,n} \left(\frac{\alpha_{m,n}}{-ik_o} \right) \exp(\alpha_{m,n} z) - A'_{m,n} \left(\frac{\alpha_{m,n}}{-ik_o} \right) \exp(-\alpha_{m,n} z) \right] \cdot \sum_j B_{j,m,n} \exp(2\pi i j x/P). \tag{11}$$

With the tangential components of the incident field given by:

$$E_y^I = E_o^I \exp(ik_o z) \tag{12a}$$

$$H_x^I = -E_o^I \exp(ik_o z), \tag{12b}$$

the tangential components of the reflected field by:

$$E_y^R(x,z) = \sum_j E_j^R \exp\left\{ -ik_o \left[\left(\frac{\lambda j}{P} \right) x + K_j^R z \right] \right\} \tag{13a}$$

$$H_x^R(x,z) = \sum_j K_j E_j^R \exp\left\{ -ik_o \left[\left(\frac{\lambda j}{P}\right) x + K_j^R z \right] \right\} , \qquad (13b)$$

where $K_j^R = \sqrt{1 - \left(\frac{\lambda j}{P}\right)^2}$

and the tangential components of the transmitted field by:

$$E_y^T(x,z) = \sum_j E_j^T \exp\left\{ ik_o \left[\left(\frac{\lambda j}{P}\right) x + K_j^T z \right] \right\} \qquad (14a)$$

$$H_x^T(x,z) = \sum_j -K_j^T E_j^T \exp\left\{ ik_o \left[\left(\frac{\lambda j}{P}\right) x + K_j^T z \right] \right\} \qquad (14b)$$

where $K_j^T = \sqrt{\hat{n}_s^{\,2} - \left(\frac{\lambda j}{P}\right)^2}$ and $\hat{n}_s$ is the complex index of the substrate.

For each Fourier component j, the following boundary equations must be satisfied:

1. At <u>z=0 (x=y=0)</u>, the solution must match the tangential

components of the <u>E</u>- and <u>H</u>-fields at the top surface:

$$E_o^I \delta_{j0} + E_j^R = \sum_m \left[A_{m,1} + A'_{m,1} \right] B_{j,m,1}; \qquad (15a)$$

$$-E_o^I \delta_{j0} + K_j^R E_j^R = \sum_m \left[A_{m,1} \left(\frac{\alpha_{m,1}}{-ik_o}\right) - A'_{m,1} \left(\frac{\alpha_{m,1}}{-ik_o}\right) \right] B_{j,m,1},$$

where $\delta_{j0} = \begin{cases} 1 & j = 0 \\ 0 & j \neq 0. \end{cases}$

2. At the interface between the n-th and (n+1)-th layer, $z = -Z_n$ (x=y=0), the $\underline{E}$- and $\underline{H}$-fields must satisfy the boundary conditions at each interface:

$$\sum_m \left[A_{m,n} \exp(\alpha_{m,n} Z_n) + A'_{m,n} \exp(-\alpha_{m,n} Z_n) \right] B_{j,m,n} \tag{16a}$$

$$= \sum_m \left[A_{m,n+1} \exp(\alpha_{m,n+1n}) + A'_{m,n,1} \exp(-\alpha_{m,n+1} Z_n) \right] B_{j,m,n+1} ;$$

$$\sum_m \left[A_{m,n} \left(\frac{\alpha_{m,n}}{-ik_o} \right) \exp(\alpha_{m,n} Z_n) - A'_{m,n} \left(\frac{\alpha_{m,n}}{-ik_o} \right) \exp(-\alpha_{m,n} Z_n) \right] B_{j,m,n}$$

$$= \sum_m \left[A_{m,n+1} \left(\frac{\alpha_{m,n+1}}{-ik_o} \right) \exp(\alpha_{m,n+1} Z_n) \right.$$

$$\left. - A'_{m,n+1} \left(\frac{\alpha_{m,n+1}}{-ik_o} \right) \exp(-\alpha_{m,n+1} Z_n) \right] B_{j,m,n+1} . \tag{16b}$$

3. At $z = -Z_N = -T$ (x=y=0), the solution must satisfy the boundary conditions imposed by the substrate (assumed infinite in extent - see Fig. 3):

$$\sum_m \left[A_{m,N} \exp(\alpha_{m,N} T) + A'_{m,N} \exp(-\alpha_{m,N} T) \right] B_{j,m,N} \tag{17a}$$

$$= E^T_j \exp(-ik_o K^T_j T) ;$$

$$\sum_m \left[A_{m,N} \left(\frac{\alpha_{m,N}}{-ik_o} \right) \exp(-\alpha_{m,N} T) - A'_{m,N} \left(\frac{\alpha_{m,N}}{-ik_o} \right) \exp(\alpha_{m,N} T) \right] B_{j,m,N}$$

$$= -K^T_j E^T_j \exp(-ik_o K^T_j T) . \tag{17b}$$

In matrix notation,

$$\begin{pmatrix} E_x^{IR} \\ H_y^{IR} \end{pmatrix} = \begin{pmatrix} B_1(0) \end{pmatrix} \cdot \begin{pmatrix} A_1 \\ A_1' \end{pmatrix} \qquad (18a)$$

$$\begin{pmatrix} B_n(Z_n) \end{pmatrix} \cdot \begin{pmatrix} A_n \\ A_n' \end{pmatrix} = \begin{pmatrix} B_{n+1}(Z_n) \end{pmatrix} \cdot \begin{pmatrix} A_{n+1} \\ A_{n+1}' \end{pmatrix} \qquad (18b)$$

$$\begin{pmatrix} B_N(T) \end{pmatrix} \cdot \begin{pmatrix} A_N \\ A_N' \end{pmatrix} = \begin{pmatrix} E_x^T \\ H^T{}_y \end{pmatrix} \qquad (18c)$$

where

$$B_n(Z_n) = \begin{pmatrix} B_n^{11}(Z_n) & B_n^{12}(Z_n) \\ B_n^{21}(Z_n) & B_n^{22}(Z_n) \end{pmatrix}$$

and the matrix elements are given by

$$B_{j,m,n}^{11}(Z_n) = \exp(-\alpha_{m,n}Z_n)B_{j,m,n}$$

$$B_{j,m,n}^{12}(Z_n) = \exp(\alpha_{m,n}Z_n)B_{j,m,n}$$

$$B_{j,m,n}^{21}(Z_n) = \left(\frac{\alpha_{m,n}}{-ik_o}\right)\exp(-\alpha_{m,n}Z_n)B_{j,m,n}$$

$$B_{j,m,n}^{22}(Z_n) = -\left(\frac{\alpha_{m,n}}{-ik_o}\right)\exp(\alpha_{m,n}Z_n)B_{j,m,n}$$

Depending upon whether the solution for the transmitted or reflected field is desired, all of the A_n and A_n's are eliminated from these equations except for either A_N and A_N' or A_1 and A_1', i.e., for the transmitted field:

$$\begin{pmatrix} A_1 \\ A_1' \end{pmatrix} = \left(B_1(Z_1)\right)^{-1} \cdot \left(B_2(Z_1)\right) \cdot \left(B_2(Z_2)\right)^{-1} \cdots \tag{19a}$$

$$\cdot \left(B_{N-1}(Z_{N-1})\right)^{-1} \cdot \left(B_N(Z_{N-1})\right) \cdot \begin{pmatrix} A_N \\ A_N' \end{pmatrix} = B \cdot \begin{pmatrix} A_N \\ A_N' \end{pmatrix}$$

or, for the reflected field:

$$\begin{pmatrix} A_N \\ A_N' \end{pmatrix} = \left(B_N(Z_{N-1})\right)^{-1} \cdot \left(B_{N-1}(Z_{N-1})\right) \cdot \left(B_{N-1}(Z_{N-2})\right)^{-1} \cdots \tag{19b}$$

$$\cdot \left(B_2(Z_1)\right)^{-1} \cdot \left(B_1(Z_1)\right) \cdot \begin{pmatrix} A_1 \\ A_1' \end{pmatrix} = B^{-1} \cdot \begin{pmatrix} A_1 \\ A_1' \end{pmatrix}$$

This operation replaces the multilayer structure with an equivalent layer characterized by the matrix B.

The equations are now solved as for the single layer case by eliminating the unknown E_j^R amd E_j^T to solve for the A_1s or A_Ns again depending upon whether the Fourier expansion of the reflected or transmitted field is desired. In the present paper, we compute the reflected field coefficients,

$$\begin{pmatrix} E_x^{IR} \\ H_y^{IR} \end{pmatrix} = \left(B_1(0)\right) \cdot \begin{pmatrix} A_1 \\ A_1' \end{pmatrix} \tag{20a}$$

$$\begin{pmatrix} B^{11} & B^{12} \\ B^{21} & B^{22} \end{pmatrix} \cdot \begin{pmatrix} A_1 \\ A_1' \end{pmatrix} = \begin{pmatrix} E_x^T \\ H_y^T \end{pmatrix} \tag{20b}$$

where

$$\begin{pmatrix} B^{11} & B^{12} \\ B^{21} & B^{22} \end{pmatrix} = \Big(B_N(T)\Big) \cdot B^{-1} \tag{20c}$$

Using the format of eqs. (18) this reduces to the single matrix equation:

$$\begin{pmatrix} D_{11} & D_{12} \\ D_{21} & D_{22} \end{pmatrix} \cdot \begin{pmatrix} A_1 \\ A_1' \end{pmatrix} = \begin{pmatrix} R \\ 0 \end{pmatrix} \tag{21}$$

where

$$D^{11}_{j,m} = \left[K_j^R - \left(\frac{\alpha_{m,1}}{-ik_o} \right) \right] B_{j,m,1}$$

$$D^{12}_{j,m} = \left[K_j^R + \left(\frac{\alpha_{m,1}}{-ik_o} \right) \right] B_{j,m,1}$$

$$D^{21}_{j,m} = \left[K_j^T B_{11} + B_{21} \right]$$

$$D^{22}_{j,m} = \left[K_j^T B_{12} + B_{22} \right]$$

and

$$R_j = \left[E_o^I (1 + K_j^R) \delta_{j0} \right]$$

where the desired coefficients E_j^R are found from eq. (15a)

$$E_j^R = \sum_m \left[A_{m,1} + A'_{m,1}\right] B_{j,m,1} - E_o^I \delta_{j0} \quad (22)$$

These coefficients represent the Fourier coefficients of a pseudo or equivalent (planar) object. The microscope image of the reflected field is then computed using scalar imaging theory (See Ref. 3.) with the line object reflectance function given by

$$t(x) = \sum_j E_j^R \exp(ik_o \lambda jx/P) \quad (23)$$

This method of computing both the reflected field and the corresponding microscope image requires no approximations of the type usually found, such as limits on the conductivity or slope of the surface, etc. Limitations may be imposed, however, by the computation capability available. First, the number of layers used to approximate the structure increases the computing time linearly. In most of the cases to be shown here, seven to nine layers were sufficient to produce significant results and required approximately one minute of CPU time on a Univac 1108.*

The second limitation is in the truncation of the series, i.e., the matrix sizes used in the computations. In the present case, as for a single layer [3], all of the reflected plane waves are included which have diffraction angles less than $\pm \pi/2$ in air. With $P = 12\mu m$ and $\lambda = 0.53\mu m$, 22 diffracted orders are included which requires a 45 x 45 complex eigenvalue matrix and a 90 x 90

*Certain commercial equipment, instruments, or materials are identified in this paper in order to adequately specify experimental or computational procedure. Such identification does not imply recommendation or endorsement by the National Bureau of Standards, nor does it imply that the materials or equipment identified are necessarily the best available for the purpose.

complex matrix for inversion of the B matrices in eqs. (19). This choice necessarily truncates the series which represents the field in the layers with higher refractive index. In the cases considered here, this truncation does not appear to significantly affect the results.

Also, for grating objects with $P \leq 12\mu m$, the computations are exact. However, for isolated line objects near resonances (where the thickness times index of refraction of the patterned layer is approximately equal to the wavelength), $P = 12\mu m$ is not large enough to eliminate the effect of the adjacent lines on the image. Larger matrix sizes would have to be used where $P > 12\ \mu m$ is required.

The Effect of Geometry on the Image Profile

The present method was developed primarily for the purpose of modeling the effect of nonvertical edges on the image profile. There is a very wide range of edge geometries which can be modeled, therefore, only a few key examples will be presented here in order to demonstrate trends. Figure 1 shows six basic shapes which are frequently encountered in integrated circuit processing. In order to simplify the definition of these shapes, they will be represented by a polynominal expansion which defines the width as a function of z.

$$W(z) = \sum_{j=0}^{J} X_j(z-Z_j)^j \quad , \qquad (24)$$

where J = the polynominal order,

X_j = coefficient of the j-th order, and

Z_j = offset of the j-th order.

The shapes in Fig. 1 have been restricted to fifth order polynominals ($J \le 5$). In these examples it will be assumed that the patterned layer is 0.6 µm thick, and the nominal linewidth X_0 is 6.0 µm. The line consists of loss-free silicon dioxide with a real refractive index of 1.46. The substrate is taken to be silicon with a complex refractive index of $4.1 + 0.06i$ at an illumination wavelength of 0.53 µm. The diffraction-limited images have been computed for a 0.14 NA illumination aperture and 0.85 NA objective aperture. Note that in this polynominal representation of the line object, although X_0 as shown in Fig. 1 is the nominal linewidth, X_0 is: the width at the top ($z=0$) in cases (b) and (g); the width at the bottom ($z=d$) in cases (c), (d), and (f), and the mean width in cases (e) and (h). Figure 4 shows the theoretical image intensity profile of an ideal line with vertical edge walls. The oxide line extends from -3.0 to +3.0 µm as shown by the dashed lines, and the rest of the object is bare silicon. In the calculation of the Fourier series coefficients, this structure is assumed to be repeated with a period of 12.0 µm. The line edge image is characterized by a dark fringe wider than the interference fringe that would be calculated for a similar thin layer.

The set of image profiles in Fig. 5 demonstrates the effect of different edge geometries on the image. The line has been assumed to be symmetrical and so only half the image profile is shown. The line objects are defined in terms of Eq. (2) and the width of the line edge is getting progressively broader down each of the three columns. There are two effects which are common to all three geometries. As the edge becomes broader, the dark fringe associated with the edge also becomes broader with the bright fringes on either side becoming brighter than occurs with partially coherent imaging of planar objects. When the edge becomes very broad, the dark fringe itself begins to broaden out and small peaks form within it.

According to the method described so far, the object is assumed to consist of homogeneous slabs of materials. This assumption is implicit in Eq. (1). In practice many materials such as polycrystalline silicon cannot be regarded as homogeneous as they have a definite internal structure which will result in a variation in refractive index within the material. These structures can be modeled by representing the random refractive index disturbances within the material by functions.

$$\hat{\varepsilon}_n'(x) = \hat{\varepsilon}_n(x) + \sum_{j=1}^{J} C_j \delta(x - X_j) \ , \qquad (25)$$

where:

$\hat{\varepsilon}_n(x)$ = refractive index profile from Eq. (1),
C_j = amplitude of j-th refractive index disturbance, and
X_j = position of j-th disturbance.

The function $\hat{\varepsilon}_n(x)$ now describes a noisy layer, and by restricting the range of values for X_j, the noise may be confined to different parts of the layer.

Figure 6 shows three image profiles for a noisy structure. The object is the oxide structure used to produce the profile in Fig. 4 and noise has been added to the entire layer. In each of the three cases shown in Fig. 6, different sets of noise data have been used corresponding to different sets of C_j selected from a random number table. The most striking feature of these curves is that, although the field is perturbed within the area of the object, the dark fringe at the edge of the line remains well defined, and relatively unperturbed.

Comparison with Experimental Results

In order to test the model against experimental image profiles, a test specimen was prepared which consisted of lines patterned in photoresist on a silicon substrate. The same test pattern was put down repeatedly by projection printing but with a range of focus positions. This produced a series of patterns with a range of edge slopes. Two patterns were selected to illustrate different edge properties. One pattern corresponded to the in-focus exposure and had near vertical edge walls; the second corresponded to a considerable defocus on exposure and had significantly sloping edges.

The in-focus exposure was assumed to produce near vertical edge walls, and when the structures were examined in a scanning electron microscope, this was found to be the case. The edge walls had slopes of about 80°, which according to the theory may effectively be assumed to be vertical for films of submicrometer thickness. The width of the window in the resist was taken as 2.5 µm.

The out-of-focus pattern had significant edge slopes, and the structure was modeled by the asymmetric third order window shown in Fig. 7, based on SEM pictures of the cross section. The photoresist thickness was not known exactly but was nominally 1 µm. The refractive index of the resist is not known exactly, but this is not serious as small changes in the refractive index can be offset by small adjustments in the layer thickness without significantly changing the image profile. The refractive index of the photoresist was assumed to be 1.513. The theoretical layer thickness was adjusted until it produced the same contrast as the experimental data; this gave a thickness for the resist of 0.94 µm.

It is very difficult to accurately determine the position corresponding to "best focus" when viewing these thick structures in

the optical linewidth measurement system. Therefore, it is necessary to generate a series of profiles as a function of focus position and compare these with the theoretical data. Figure 8 shows a comparison of the experimental and theoretical image profiles produced by these structures. The experimental data were generated using the coherent optical linewidth measurement system which has been described in detail in the literature by Nyyssonen.[3]

The profiles for the sloping edge structure are quite different from those for the vertical edge structure. However, in both cases they show good agreement with the models. The theoretical profiles display the same features as the experimental profiles, but the agreement is not perfect. One significant source of differences is the assumption that the resist is homogeneous. This is not strictly true. To get better agreement, it would have been advantageous to use a material such as silicon dioxide which is homogeneous and which would produce a stable and accurately known refractive index.

A second source of differences may arise from the assumption that the illumination is normally incident. As shown in the experimental data, the central peak of the sloping edge profile moves as the object moves through focus and the line with nearly vertical edges generates slightly asymmetric profiles (See Fig. 8). Both of these may be attributed to slight asymmetry in either the illumination system or imaging optics. The NBS profiling system used to generate these profiles was checked for illumination symmetry when profiling thin layers. However, it is expected that these thick layers are significantly more sensitive to asymmetric illumination than is a thin-layer object.

Case Study of the Production of an MOS Transistor

This section considers some typical structures which are encountered in microlithography and the effect of small variations in

these structures on the optical image profile. The two structures shown in Fig. 9 are considered. These structures represent the key stages of patterning the polysilicon layer when making an MOS device. The structure in Fig. 9(a) represents the stage between patterning the resist and etching the polysilicon. Controlling the resist dimensions at this stage will help control the final etched polysilicon linewidth. However, measuring the width of the resist line at this stage is difficult because the image profile is a function of the geometry, refractive index, and thickness of each of the three layers. The polysilicon was assumed to have a refractive index of $3.8 + 0.1i$.

The curves in Fig. 10 show how variations in the thickness of the polysilicon affect the image profile of the resist line. Again, only half the image profile is shown. The most striking feature of these curves is that the image structure in the immediate vicinity of the line edge is sensitive to the thickness of the polysilicon layer.

The structure in Fig. 11 represents a polysilicon line after etching and stripping of the resist. The image profile is a function of the thickness of the silicon-dioxide layer. Figure 12 shows the effect of changing the thickness of the oxide sublayer on the image profile of the structure shown in Fig. 9(b). The polysilicon is assumed in this case to have vertical edge walls and the oxide thickness is varied over a range of 40 nm. As the thickness changes, the image profile changes considerably. This makes linewidth measurement difficult as there appears to be no feature or threshold which locates the edge independently of oxide thickness.

The image profile is also a function of edge geometry and in Fig. 9(b) it has been assumed that the edge shape can be defined by a second order polynomial with the polynomial of Eq. (2) given by

$$W(z) = X_0 + X_2 . z^2 , \tag{26}$$

where, again, the nominal linewidth X_0 is 6.0 µm. The curves in Fig. 12 show the effect of variations in the edge curvature of the polysilicon layer on the image profile. The edge image profile is clearly sensitive to the curvature of the physical edge of a curved feature. In this case, three possible definitions of linewidth are the minimum, maximum, or mean width of the layer. For the examples shown in Fig. 12, these definitions all give linewidths which do not correspond to that given by the position of the minimum of the dark fringe. More importantly, however, the offset between the true and measured linewidth varies with the degree of curvature over a range of a few tenths of a micrometer regardless of the definition used for the line edge.

Summary

A waveguide model has been presented which enables the optical images of line structures patterned in thick layers to be computed. The model has been shown to be applicable to a wide range of structures, and qualitative agreement with experimental image profiles has been demonstrated. From the results presented here, it can be seen that the image profile of a thick line object, and therefore the measured linewidth, is affected by the physical shape of the edges.

The model enables the effects of process variations on the optical image profile to be determined and this, in turn, enables the accuracy and sensitivity of different measurement techniques to be investigated. Further work is in progress to improve existing measurement methods in order to minimize the effects of process variations on the accuracy and repeatability of linewidth measurements.

Acknowledgments

The authors wish to acknowledge the help of Marilyn J. Dodge who collected the experimental image profiles for this work. This work was carried out as part of one of the author's (Kirk) Ph.D. research program supported by the Science and Engineering Research Council (UK).

Appendix

In matrix notation, the eigenvalue problem of eq. (9) is:

$$D \cdot B_n = \alpha^2 I \cdot B_n$$

where the matrix elements $D_{i,j}$ for the n-th layer are given by

$$D = \begin{pmatrix}
-(E_{o,n}+K_j^2) & E_{1,n} & \cdots & E_{i-j,n} & 0 & \cdots & 0 \\
E_{1,n} & \ddots & & \vdots & \ddots & & \vdots \\
\vdots & & \ddots & E_{1,n} & & \ddots & 0 \\
E_{i-j,n} & \cdots & E_{1,n} & -(E_{o,n}+K_o^2) & E_{1,n} & \cdots & E_{i-j,n} \\
0 & \ddots & & E_{1,n} & \ddots & & \vdots \\
\vdots & & \ddots & \vdots & & \ddots & E_{1,n} \\
0 & \cdots & 0 & E_{i-j,n} & \cdots & E_{1,n} & -(E_{o,n}+K_j^2)
\end{pmatrix}$$

and $K_j = \dfrac{\lambda j}{P}$

References

1. M. Born and E. Wolf, Principles of Optics, 5th ed., (Pergamon Press, Oxford, 1975), pp. 522-532.

2. L. C. Martin, The Theory of the Microscope, (Blackie, London, 1966), Chapters V and VIII.

3. D. Nyyssonen, "Theory of optical edge detection and imaging of thick layers", J. Opt. Soc. Am. 72, pp. 1425-1436 (1982).

4. Ref. 1, Section 13.5, pp. 633-664.

5. P. W. Barber, D. Y. Wang, and M. B. Long, "Scattering calculations using a microcomputer," App. Opt. 20, 1121-1123 (1981).

6. J. P. Hugonin and R. Petit, "Theoretical and numerical study of a locally deformed stratified media," J. Opt. Soc. Am. 71, 664-674 (1981).

7. R. Petit, ed., Electromagnetic Theory of Gratings, (Springer-Verlag, Berlin, 1980).

8. K. A. Zaki and A. R. Neureuther, "Scattering from a perfectly conducting surface with sinusoidal height profile, TE polarization," IEEE Trans. Antennas. Propagat. AP-19, 208-214 (1971).

9. J. P. Hugonin, R. Petit, and M. Cadilhac, "Plane-wave expansions used to describe the field diffracted by a grating," J. Opt. Soc. Am. 71, 593-598 (1981).

10. Ref. 1, p. 453.

11. D. Nyyssonen, "Optical linewidth measurement on patterned metal layers," Proc. SPIE 480, Integrated Circuit Metrology II, 65-70 (1984).

12. C. B. Burckhardt, "Diffraction of a plane wave at a sinusoidally stratified dielectric grating", J. Opt. Soc. Am. 56, pp. 1502-1509 (1966).

13. F. G. Kaspar, "Diffraction by thick, periodically stratified gratings with complex dielectric constant," J. Opt. Soc. Am. 63, 37-45 (1973). 14. F. G. Kaspar, "Computation of light transmitted by a thick grating, for application to contact printing," J. Opt. Soc. Am. 64, 1623-1630 (1974).

15. W. Magnus and S. Winkler, Hill's Equation (John Wiley and Sons, New York, 1966 and Dover, New York, 1979).

16. Ref. 1, p. 612.

17. Ref. 1, p. 579.

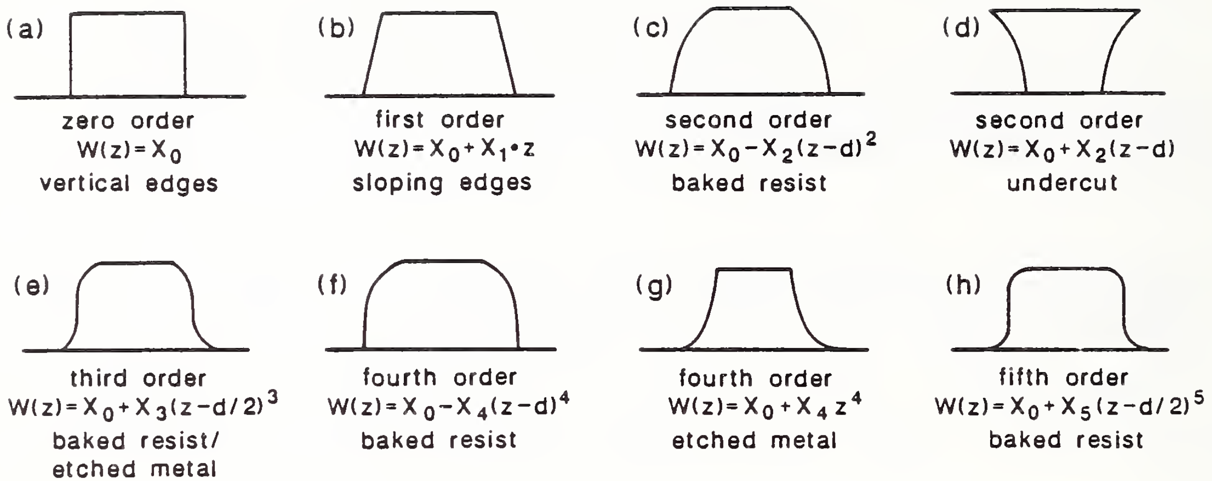

Fig. 1. The geometry of most line objects encountered in integrated circuits may be approximated by low order polynomials.

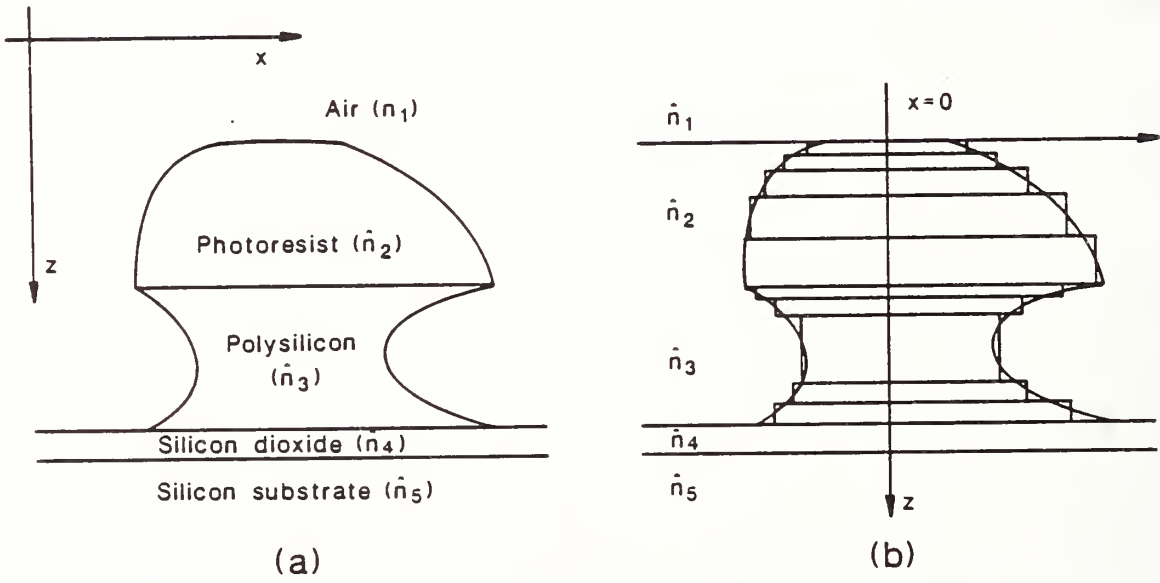

Fig. 2. Cross section of a hypothetical thick line object (a) and the corresponding multi-layer representation (b).

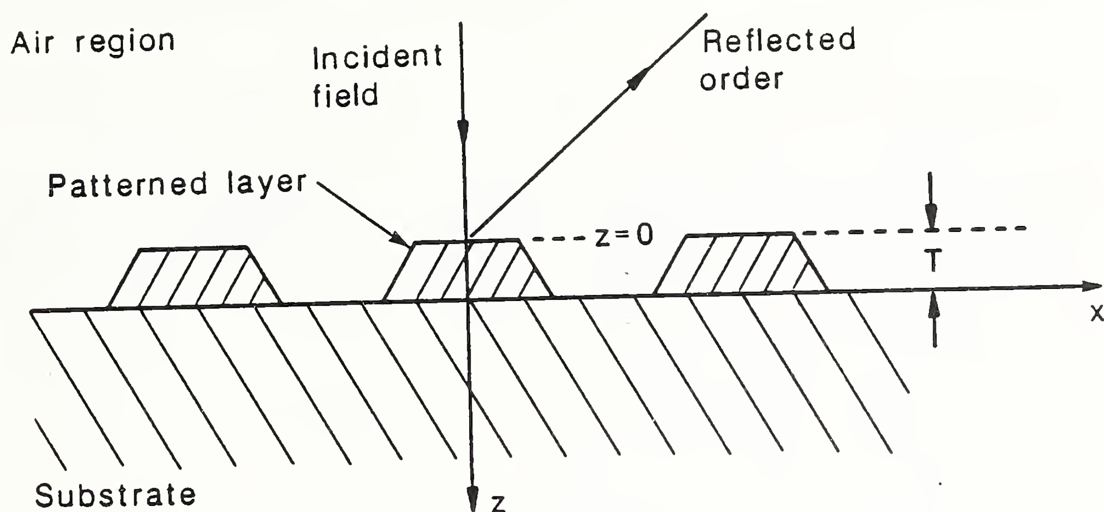

Fig. 3. Orientation of the line structure and incident fields in the NBS linewidth measuring system. The y-direction is out of the page and parallel to the length of the line patterns.

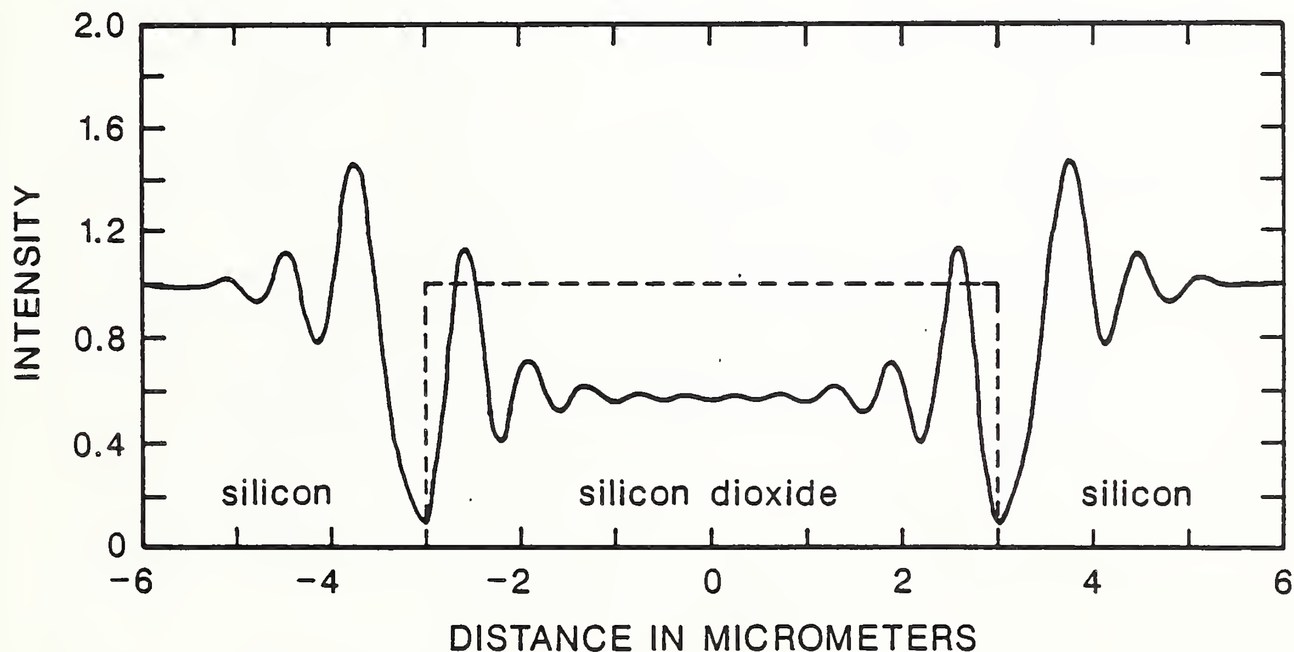

Fig. 4. Theoretical image intensity profile of a 6.0 µm wide line centered at zero, patterned in a 0.6 µm thick SiO_2 layer on silicon. λ = 530 nm.

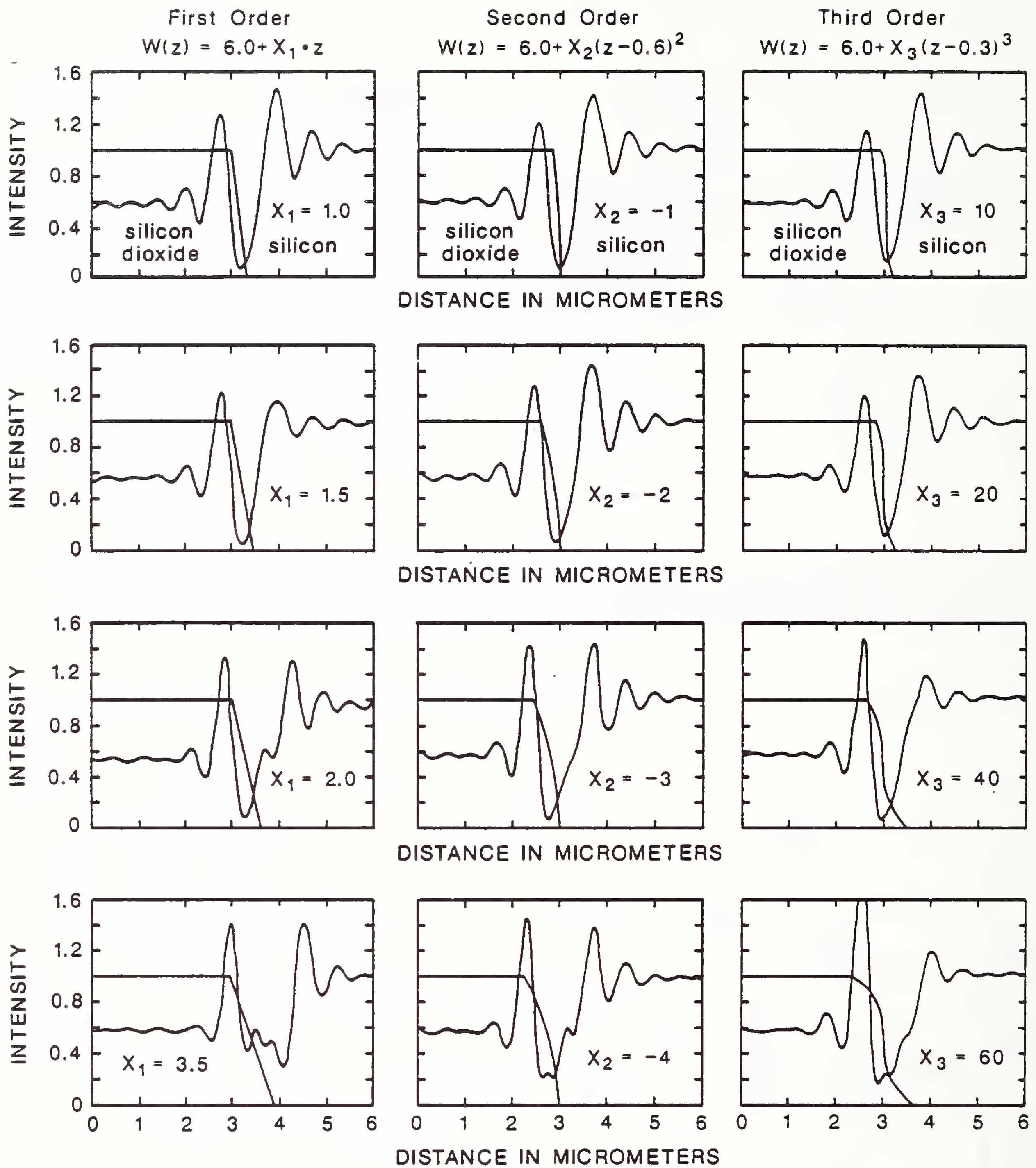

Fig. 5. The effect of edge geometry on the calculated optical image profile. The edge geometry has been superimposed on the image profile for reference.

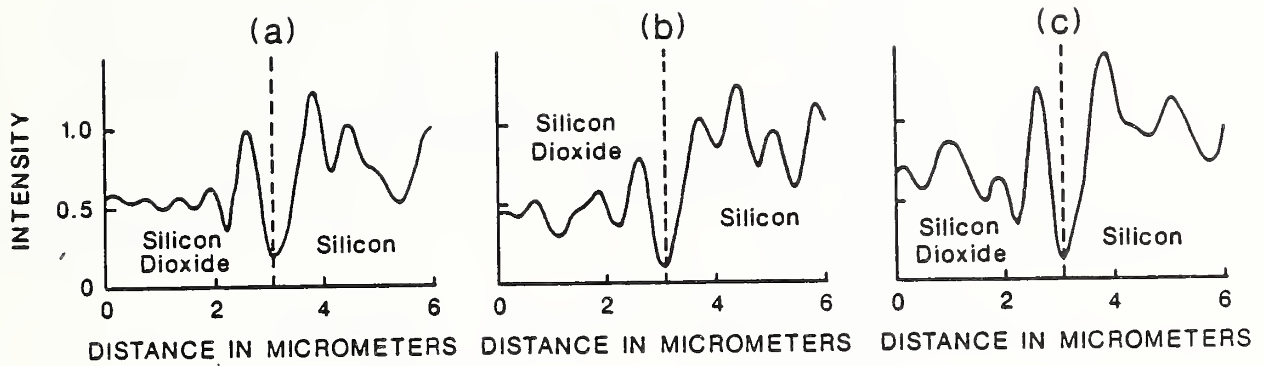

Fig. 6. Theoretical image intensity profiles of a line patterned in a noisy dielectric layer on silicon. A different set of noise data has been used for each curve.

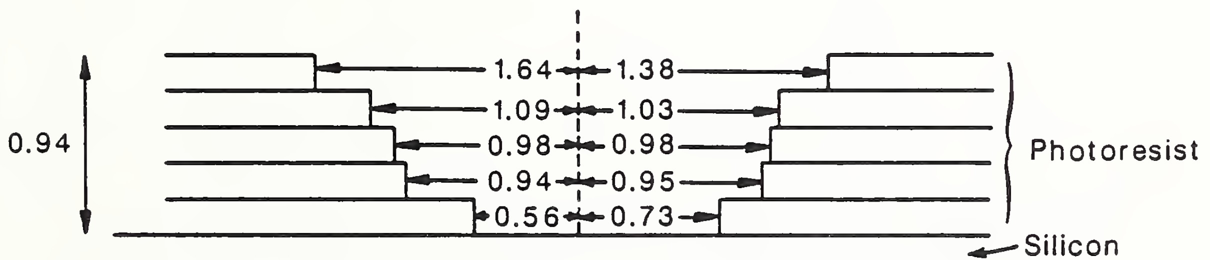

Fig. 7. Physical profile model of the asymmetric window structure in resist used to compute the image profiles in Fig. 8. (Dimensions in micrometers.)

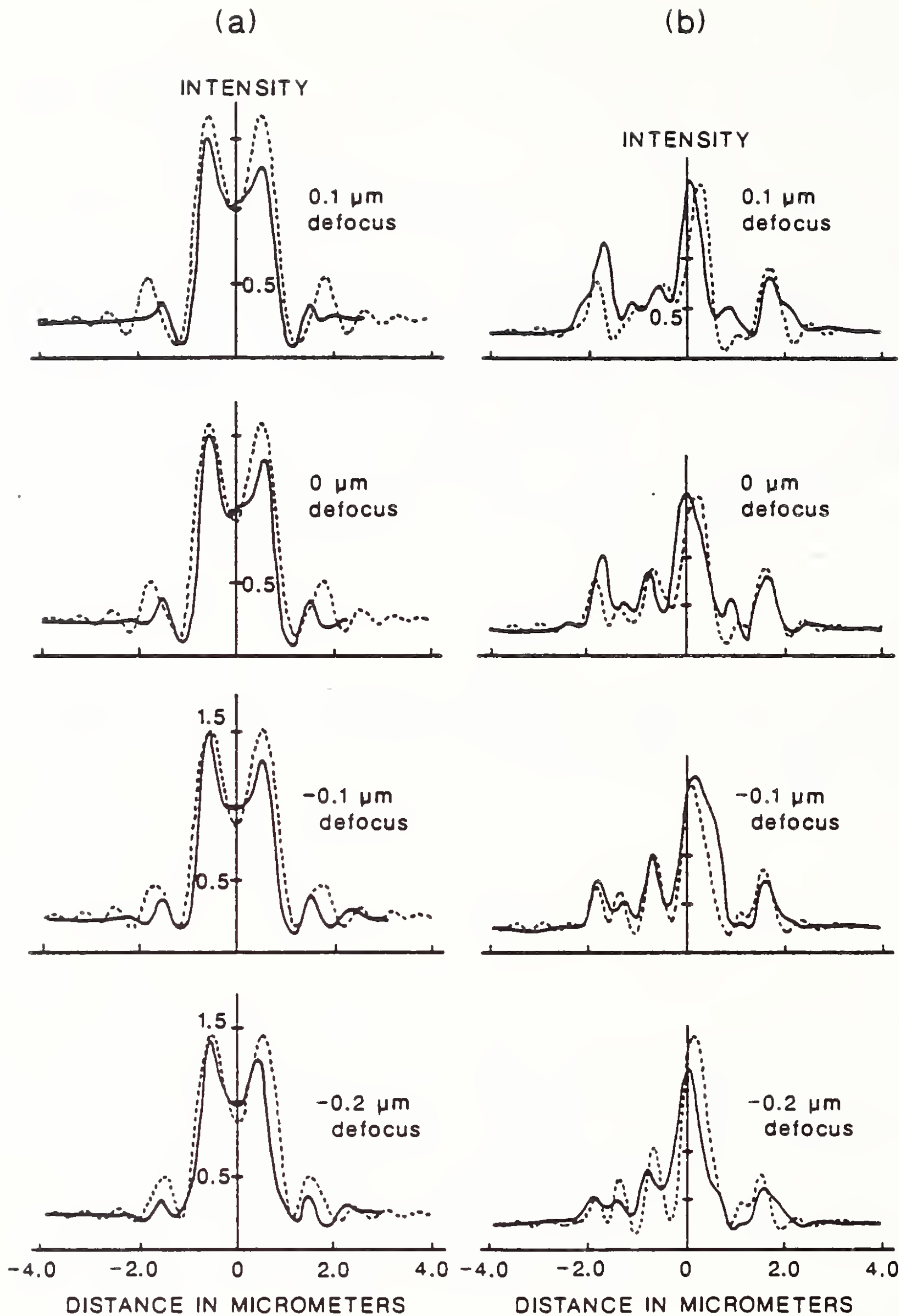

Fig. 8. Comparison of experimental and theoretical image intensity profiles of a window in photoresist on silicon. The window has either vertical edge walls (a) or sloping edges (b). The experimental profiles are shown by the thick line and the theoretical profiles by the thin line. The photoresist was assumed to have a thickness of 0.94 µm and the geometry shown in Fig. 7 was used to model the window in the case of sloping edges.

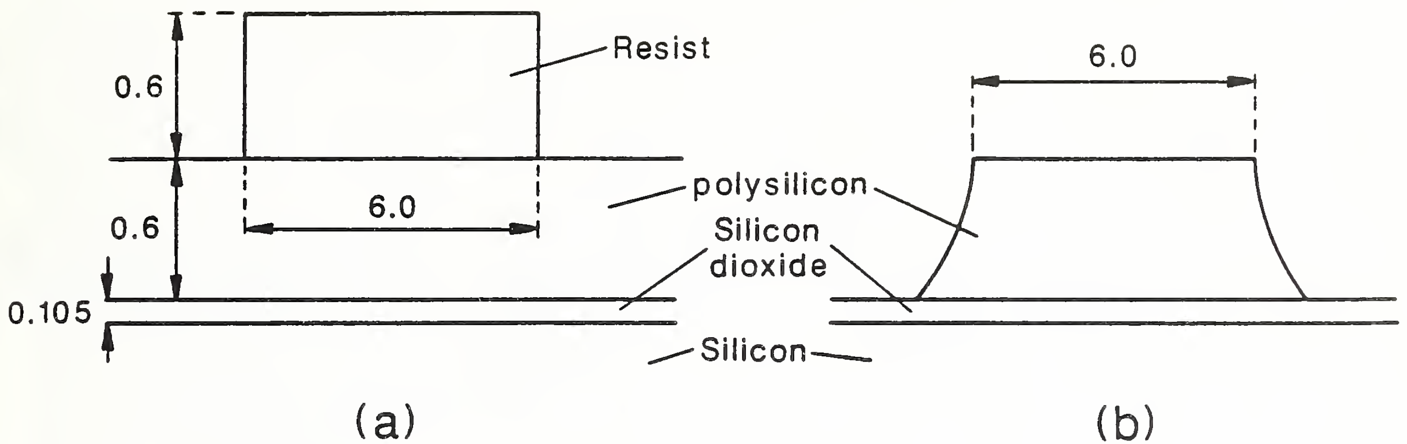

Fig. 9. Cross sections of the shapes used to model the polysilicon patterning stage of making an MOS transistor. The two shapes are patterned resist in unetched polysilicon (a) and etched polysilicon with the resist removed (b). (Dimensions in micrometers.)

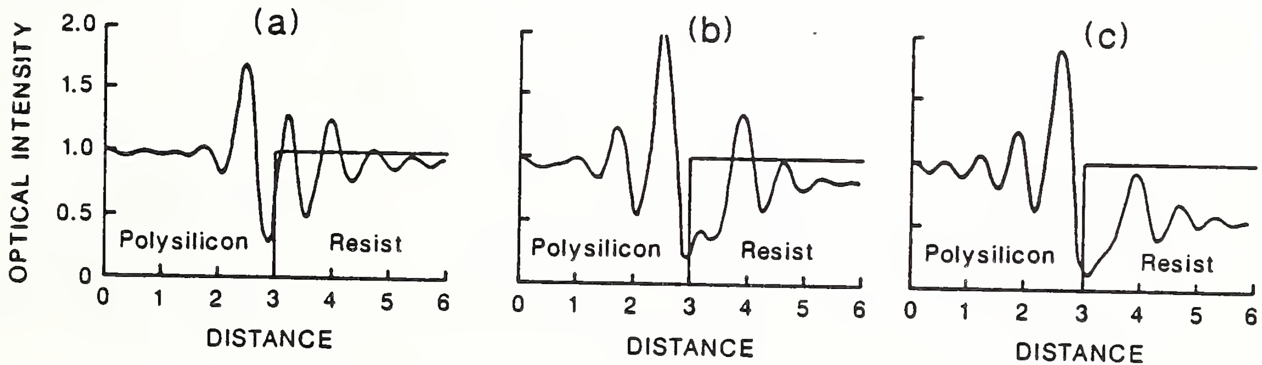

Fig. 10. Theoretical image profiles of a resist line on polysilicon (structure in Fig. 9a) for polysilicon thicknesses of a) 0.5, b) 0.6, and c) 0.7 µm. A vertical edge is assumed.

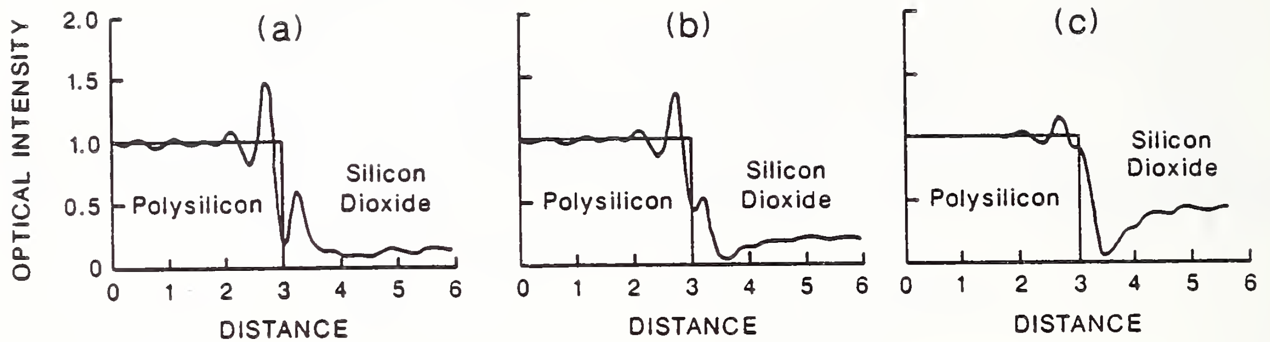

Fig. 11. Theoretical image profiles of a polysilicon line (structure in Fig. 9b) for oxide thicknesses of a) 85, b) 105, and c) 125 nm. A vertical edge is assumed and 0.6 μm polysilicon thickness.

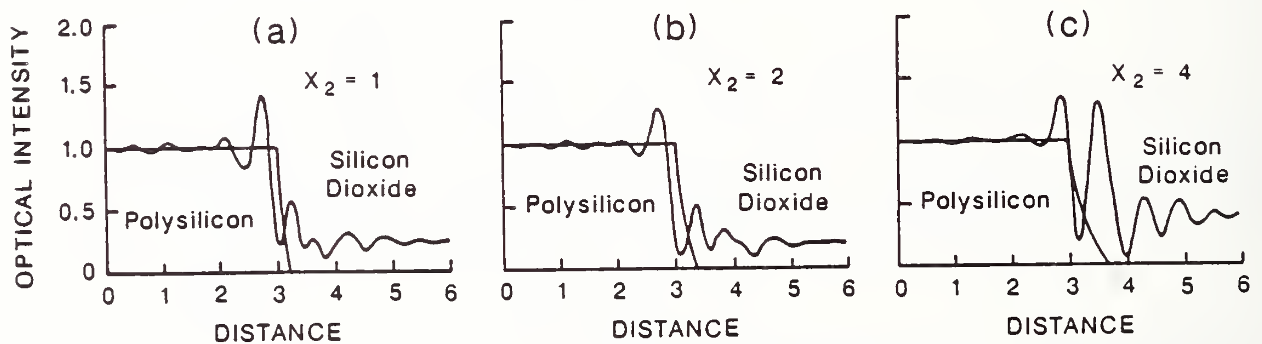

Fig. 12. Theoretical image profiles of a polysilicon line (structure in Fig. 9b) for a range of edge curvatures defined by Eq. 26. Oxide thickness is 105 nm; polysilicon thickness is 0.6 μm.

FEDERAL INFORMATION PROCESSING STANDARD SOFTWARE SUMMARY

01. Summary date (Yr. Mo. Day): 87 11 06

02. Summary prepared by (*Name and Phone*): Diana Nyyssonen (301)975-2099

03. Summary action: New [X] Replacement [ ] Deletion [ ]

Previous Internal Software ID

04. Software date (Yr. Mo. Day): 87 08

05. Software title: THKIMAG - Computer software for the computation of optical microscope images of line objects patterned in thick layers viewed in a coherent system.

06. Short title: THKIMAG

07. Internal Software ID

08. Software type:
- [ ] Automated Data System
- [X] Computer Program
- [ ] Subroutine/Module

09. Processing mode:
- [ ] Interactive
- [X] Batch
- [ ] Combination

10. Application area

General:
- [ ] Computer Systems Support/Utility
- [X] Scientific/Engineering
- [ ] Bibliographic/Textual
- [ ] Management/Business
- [ ] Process Control
- [ ] Other

Specific: Optical imaging

11. Submitting organization and address

National Bureau of Standards
Microelectronics Dimensional Metrology Group
Precision Engineering Division, 731
Center for Manufacturing Engineering
Building 225, Rm A347

12. Technical contact(s) and phone

Robert D. Larrabee
(301)975-2298

Diana Nyyssonen
(301)975-2099

13. Narrative

This computer software calculates the optical microscope images of line objects patterned in thick layers (more than one-quarter of the illuminating wavelength thick). The algorithms used are based on a monochromatic,waveguide model which can predict the image of line objects with arbitrary cross-section geometry including multilayer structures with sloped, curved,asymmetric, and undercut edges. Along with the computer software, test cases for help in implementation are given. As written, the program uses subroutines for complex matrix eigenvalues and eigenvectors from the NAG library.

14. Keywords

diffraction; dimensional metrology; linewidth; microscopy; optical imaging; optical metrology; waveguide

15. Computer manuf'r and model	16. Computer operating system	17. Programing language(s)	18. Number of source program statements
Cyber 855 (CDC)	NOS 2 (CDC)	ANSI FORTRAN77	949

19. Computer memory requirements	20. Tape drives	21. Disk/Drum units	22. Terminals
91170 words		120K words	

23. Other operational requirements

24. Software availability: Available [X] Limited [ ] In-house only [ ]

25. Documentation availability: Available [X] Inadequate [ ] In-house only [ ]

26. FOR SUBMITTING ORGANIZATION USE

NBS-114A (REV. 2-80)

U.S. DEPT. OF COMM. BIBLIOGRAPHIC DATA SHEET (See instructions)	1. PUBLICATION OR REPORT NO. NBSIR 87 3618	2. Performing Organ. Report No.	3. Publication Date

4. TITLE AND SUBTITLE

Computer Software for the Computation of the Scattered Field and the Optical Microscope Image of Line Objects Patterned in Thick Layers

5. AUTHOR(S)

6. PERFORMING ORGANIZATION (If joint or other than NBS, see instructions)

NATIONAL BUREAU OF STANDARDS
U.S. DEPARTMENT OF COMMERCE
GAITHERSBURG, MD 20899

7. Contract/Grant No.

8. Type of Report & Period Covered

9. SPONSORING ORGANIZATION NAME AND COMPLETE ADDRESS (Street, City, State, ZIP)

10. SUPPLEMENTARY NOTES

☐ Document describes a computer program; SF-185, FIPS Software Summary, is attached.

11. ABSTRACT (A 200-word or less factual summary of most significant information. If document includes a significant bibliography or literature survey, mention it here)

This report contains computer software for calculating optical microscope images of line objects patterned in thick layers (>λ/4 thick). The algorithms used are based on a monochromatic, waveguide model which can predict the images of line objects with arbitrary edge geometry including multilayer structures with sloped, curved, asymmetric, and undercut edges. Along with the computer software listing, the mathematics of the model, a short description of its structure and use, and test cases for help in implementation are given.

12. KEY WORDS (Six to twelve entries; alphabetical order; capitalize only proper names; and separate key words by semicolons)

diffraction; dimensional metrology; linewidth; microscopy; optical imaging; optical metrology; computer software

13. AVAILABILITY

☒ Unlimited
☐ For Official Distribution. Do Not Release to NTIS
☐ Order From Superintendent of Documents, U.S. Government Printing Office, Washington, D.C. 20402.
☒ Order From National Technical Information Service (NTIS), Springfield, VA. 22161

14. NO. OF PRINTED PAGES

86

15. Price

$13.95

USCOMM-DC 6043-P80